The Origin of Type Ia Supernovae

Peter Lundqvist
Stockholm Observatory, AlbaNova

(Talk at St. Petersburg, June 27, 2008)

The Origin of Type Ia Supernovae...

Why are SNe Ia interesting?

astrophysical relevance: cosmology

- tool for geometrical survey of the universe
  - brightness
  - uniformity
  - empirical calibration
- content of the universe:
  - 70% dark energy
  - 30% matter (dark and visible)

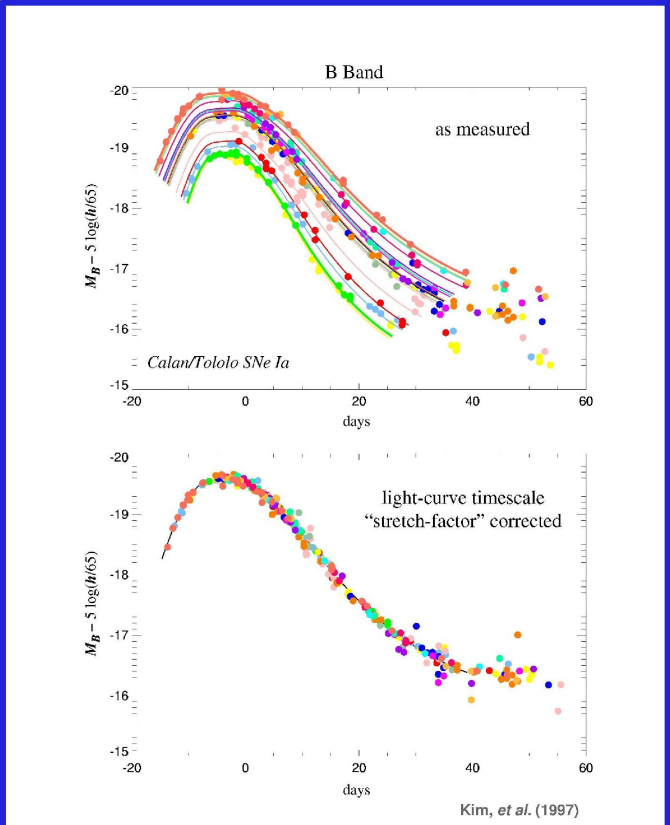

The small spread in the corrected light curve could be systematic – do we have more than one route to produce Type Ia:s?

The Origin of Type Ia Supernovae...

What are SNe Ia?

astrophysical events of enormous energy release and brightness

Favored astrophysical model:

thermonuclear explosion of a white dwarf star

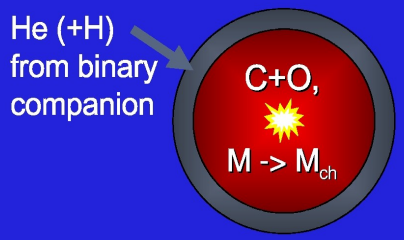

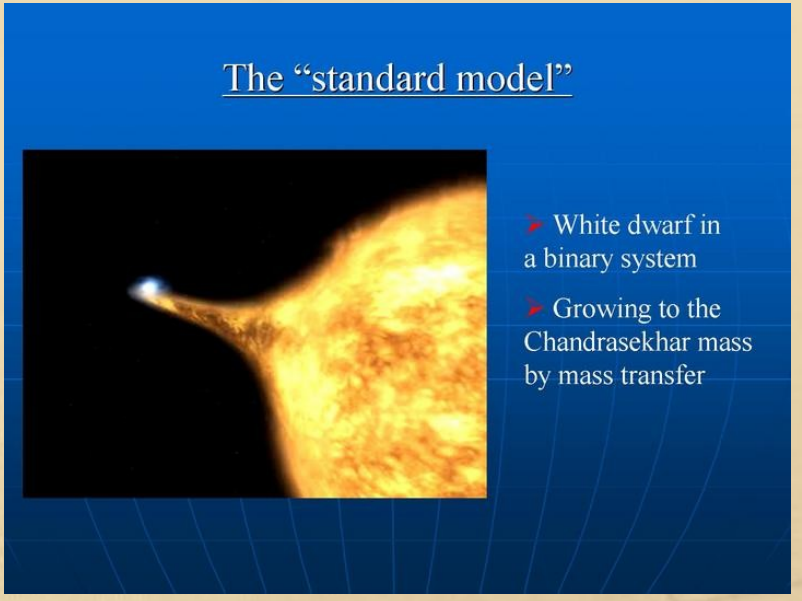

Another possibility is two merging white dwarfs.Which is the correct one?

Which single-degenerate systems could produce Type Ia SNe?

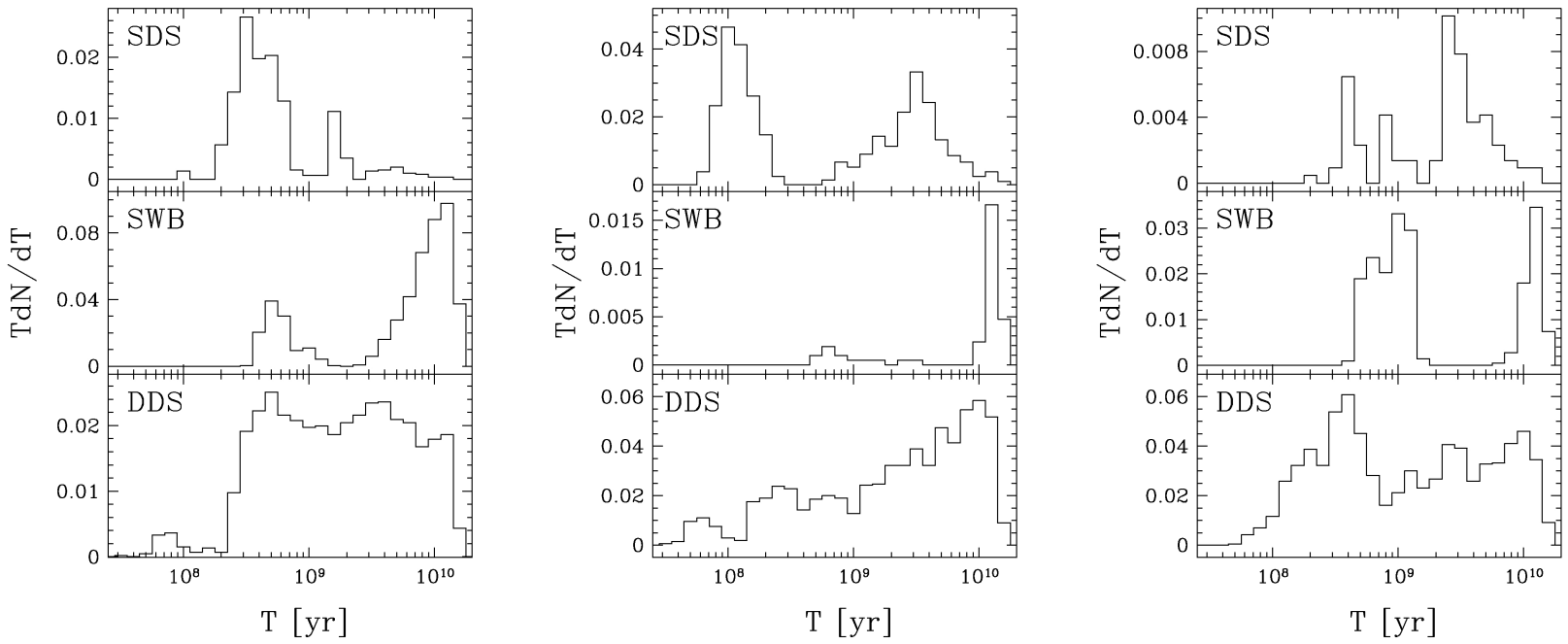

FIG. 1.—Distribution of SN Ia delay times since the burst of star formation. *Left*: Results of our standard model calculation ($\alpha\lambda = 1.0$). *Middle*: Evolution with the decreased CE efficiency ($\alpha\lambda = 0.3$) *Right*: Results for alternative CE description ($\gamma = 1.5$). The three different classes of SN Ia progenitors are shown in each panel: single-degenerate scenario (*top*), semidetached double WD binaries (*middle*), and double-degenerate scenario (*bottom*). The distributions are normalized to the sum of all SN Ia progenitors (SDS+SWB+DDS) in the model. The data are binned in the intervals with the width of 0.1 in $\log(T/\mathrm{yr})$.

(Belczynski et al. 2005)

What do SNe Ia survey programs suggest ?

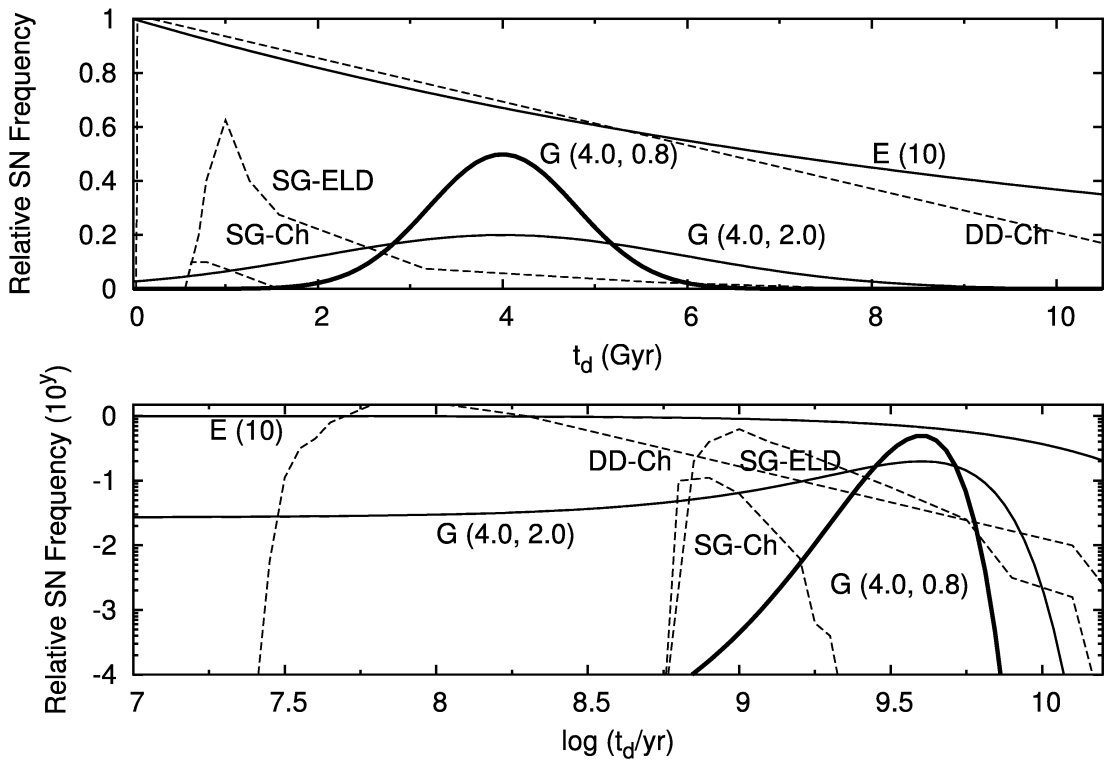

FIG. 15.—SN distributions, in linear and log space, for the maximum likelihood values of τ of each delay-time function (*solid lines*). Shown are the *e*-folding $\Phi(t_d)$ for $\tau = 10$ [E(10)], the wide Gaussian for $\tau = 4.0$ [G(4.0, 2.0)], and the narrow Gaussian for $\tau = 4.0$ [G(4.0, 0.8)]. The dashed lines represent predicted distributions of SN Ia delay times from various models (Yungelson & Livio 2000; reproduced from their Fig. 2). Shown are the predictions from double degenerate mergers (DD-Ch), edge-lit detonations from subgiant donors (SG-ELD), and normal accretion/detonations from subgiant donors (SG-Ch). There is some similarity to our best-fit models.

(Strolger et al. 2004, confirmed by Dahlen et al. 2008)

What do SNe Ia survey programs suggest ?

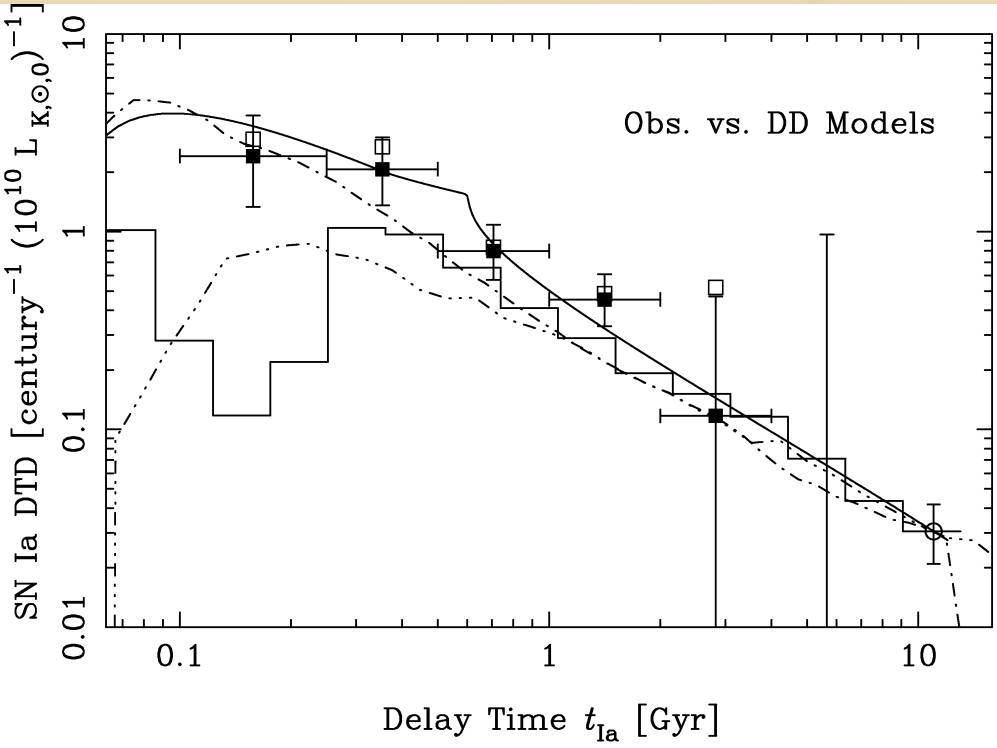

Fig. 7. The delay time distribution (DTD) of SNe Ia per unit delay time, $t_{\rm Ia}$ (century^{-1}), for a single starburst population whose total K-band luminosity is $10^{10} L_{K,\odot}$ at the age of 11 Gyr. The filled squares are the final observational estimates by this work, and the error bars are statistical 1σ errors. The open squares are the same but using a simpler method to estimate the delay time. (The error bars are not shown for these.) The open circle is DTD inferred from the SN Ia rate in elliptical galaxies in the local universe (Mannucci et al. 2005). The theoretical predictions based on the DD scenario by Ruiz-Lapuente & Canal (1998, three-dot-dashed), Yungelson & Livio (2000, dot-dashed), Greggio (2005, solid curve), and Belczynski et al. (2005, solid histogram) are also shown. The model curves are normalized by the DTD data at $t_{\rm Ia} = 11$ Gyr.

(Totani et al. 2008)

What do SNe Ia survey programs suggest ?

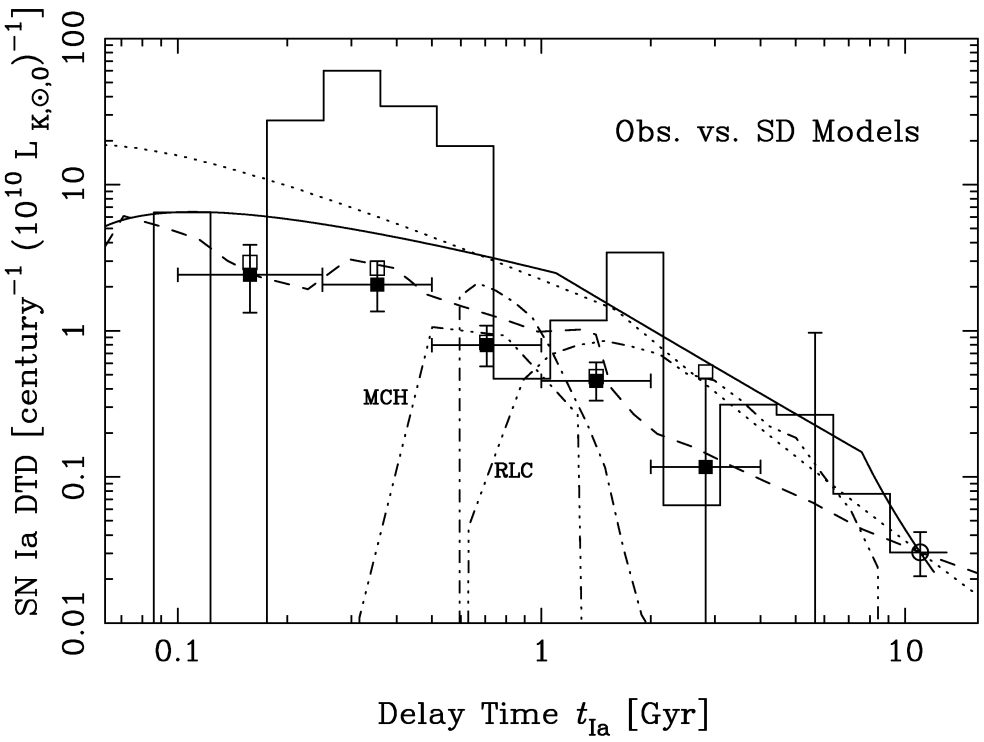

Fig. 10. The same as Fig. 7, but for a comparison with the DTD predictions based on the SD scenario. The predictions of Greggio (2005, solid curve), Matteucci et al. (2006, dotted), and Kobayashi & Nomoto (2008, dashed) are based on analytic models. The predictions of Ruiz-Lapuente & Canal (1998, three-dot-dashed with the label "RLC"), Yungelson & Livio (2000, dot-dashed), Belczynski et al. (2005, solid histogram), and Meng et al. (2008, three-dot-dashed with the label "MCH") are based on binary stellar population synthesis calculations. The model curves are normalized by the DTD data at t_{Ia} = 11 Gyr when they are non-zero, otherwise the normalization is arbitrary.

(Totani et al. 2008)

Testing non-conservative mass loss

Some of the mass might escape from the binary system.

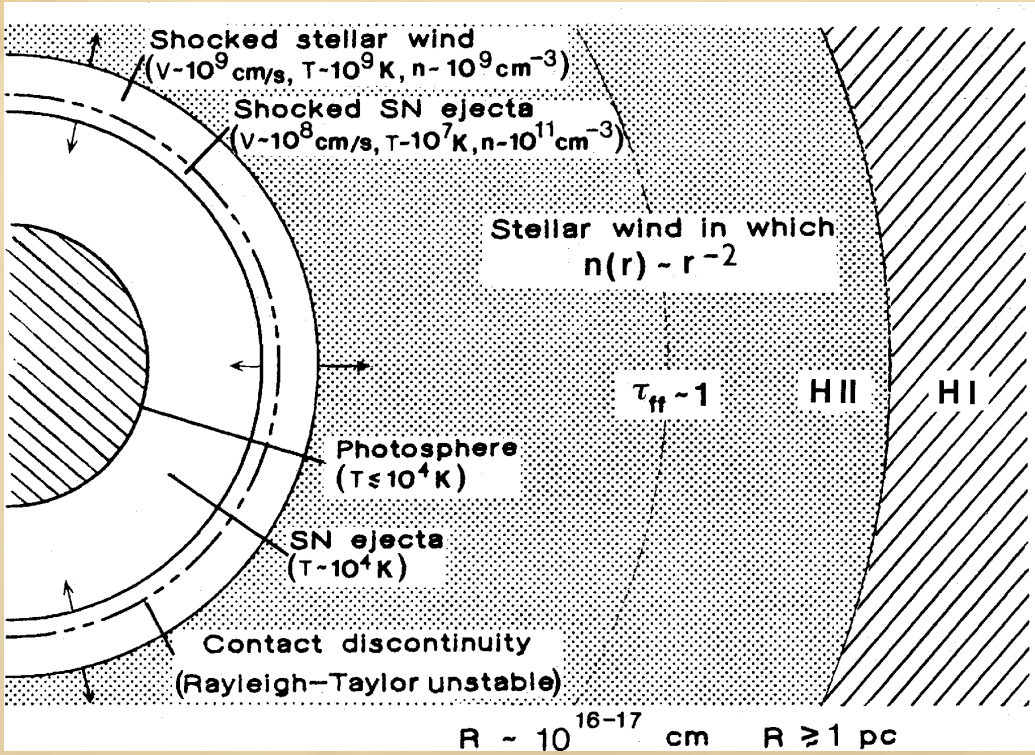

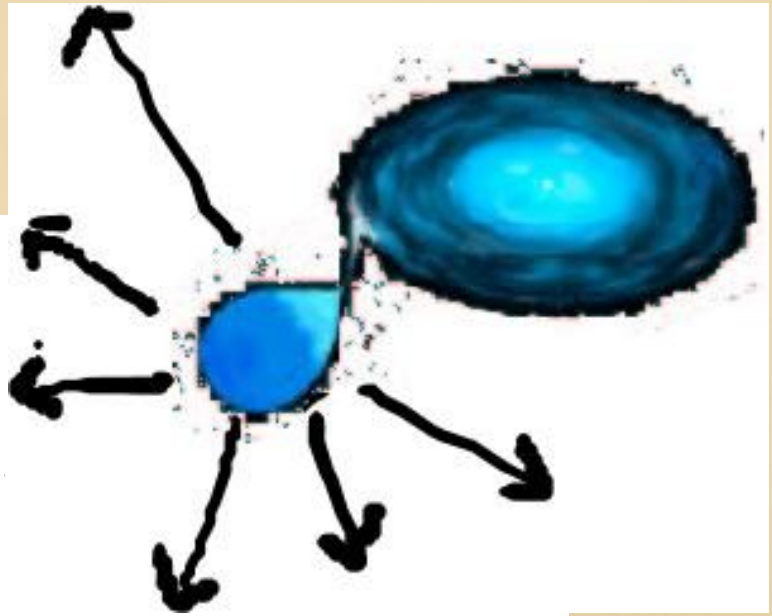

Fig. 1. Schematic picture (not to scale) of a young Type II supernova interacting with a dense circumstellar medium, originating from presupernova mass loss. Typical values of the important physical parameters are shown, as well as the boundary of the region where the free-free optical depth to the radio emission is unity and the boundary of the ionized region

We might use the same model as for young core-collapse SNe. (The companion is overtaken in just a few hours and the system quickly becomes point-symmetric.)

Model for the circumstellar interaction

SELF-SIMILAR SOLUTIONS FOR THE INTERACTION OF STELLAR EJECTA WITH AN EXTERNAL MEDIUM

ROGER A. CHEVALIER
Department of Astronomy, University of Virginia
Received 1981 October 26; accepted 1982 February 8

CIRCUMSTELLAR INTERACTION IN SN 1993J

CLAES FRANSSON AND PETER LUNDQVIST
Stockholm Observatory, S-133 36 Saltsjöbaden, Sweden
AND
ROGER A. CHEVALIER
Department of Astronomy, University of Virginia, P.O. Box 3818, Charlottesville, VA 22903
Received 1994 May 17; accepted 1995 July 14

Assume power-law dependencies on density for the ejecta, $\rho \propto r^{-n}$ and the CS gas, $\rho \propto r^{-s}$. The W7 model has roughly n=7, and the wind has s=2.

PROPERTIES OF THE SELF-SIMILAR SOLUTIONS

s	n	R_1/R_c	R_2/R_c	A	ρ_2/ρ_1	p_2/p_1	u_2/u_1	M_2/M_1
2	7	1.299	0.970	0.27	7.8	0.27	1.058	0.82
2	12	1.226	0.987	0.038	46	0.37	1.104	2.7

Numerical solution of shock structure for 3×10^{-5} M_o/yr, v_{wind}=10 km/s

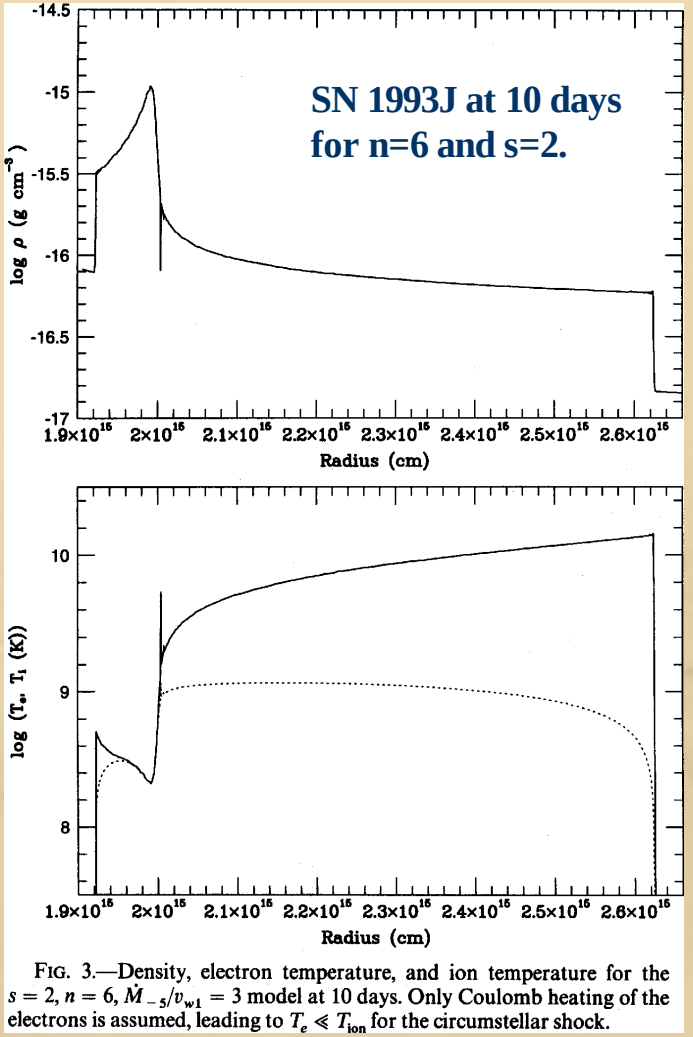

FIG. 3.—Density, electron temperature, and ion temperature for the $s = 2$, $n = 6$, $\dot{M}_{-5}/v_{w1} = 3$ model at 10 days. Only Coulomb heating of the electrons is assumed, leading to $T_e \ll T_{ion}$ for the circumstellar shock.

Ionizing Radiation

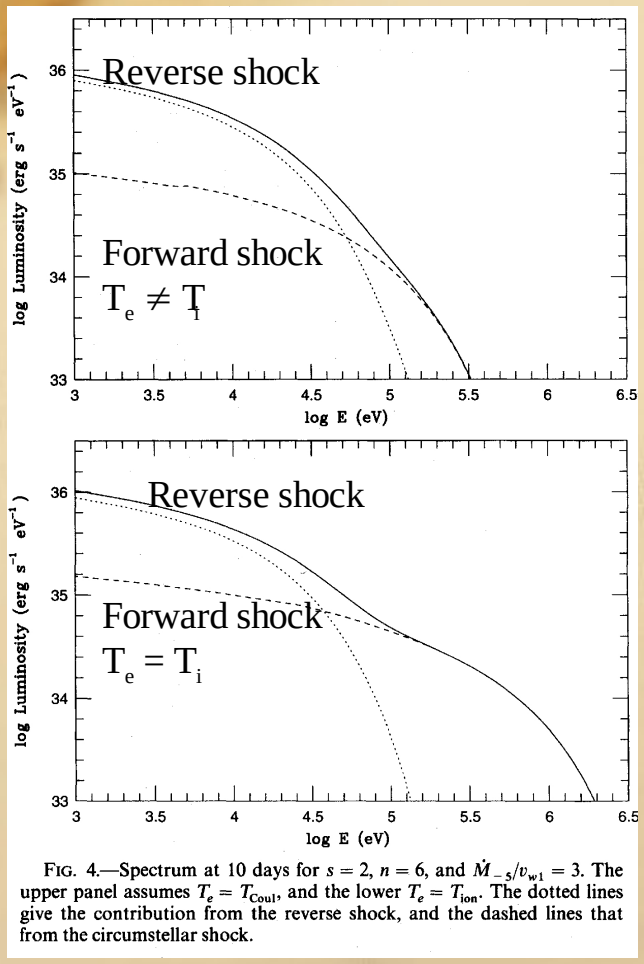

FIG. 4.—Spectrum at 10 days for $s = 2$, $n = 6$, and $\dot{M}_{-5}/v_{w1} = 3$. The upper panel assumes $T_e = T_{\rm Coul}$, and the lower $T_e = T_{\rm ion}$. The dotted lines give the contribution from the reverse shock, and the dashed lines that from the circumstellar shock.

(Fransson et al. 1996)

Consists of:

Free-free emission from the shocked ejecta (important)
Free-free emission from the shocked CS gas (not so important)
Photospheric emission and inverse Compton scattering thereof (can be very important early on)
Prompt emission from shock breakout (not so important)
Radioactive decay (can be important)
Precursor emission (can be important)

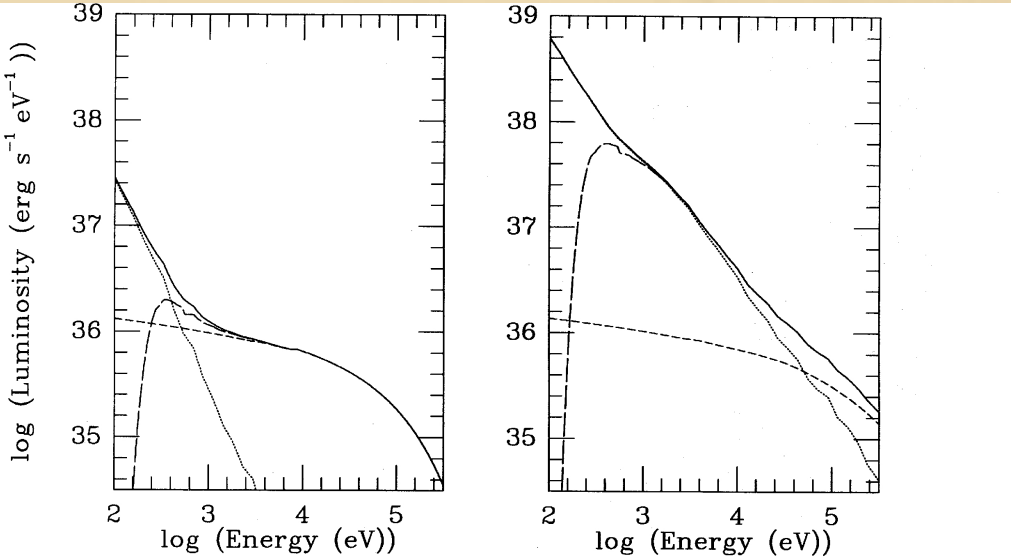

FIG. 7.—Spectrum at 10 days for the $s = 2$, $n = 25$, $\dot{M}_{-5}/v_{w1} = 4.0$ model including Comptonization of photospheric photons by the nearly relativistic electrons behind the circumstellar shock. The left-hand panel is for $T_e = T_{\rm Coul}$, and the right, for $T_e = T_{\rm ion}$. Short-dashed lines show the free-free luminosity, dotted lines, the Comptonized luminosity, and solid lines, the total luminosity. Long-dashed lines show the observable luminosity assuming an interstellar column density of 4.3×10^{20} cm^{-2}. With $T_e = T_{\rm ion}$ especially the *ROSAT* range is dominated by the Compton contribution, with a power-law slope of ~ 1.0. This is in contradiction to the observed spectrum.

Constraints on the models

Maximum velocity of the ejecta must exceed observed ones

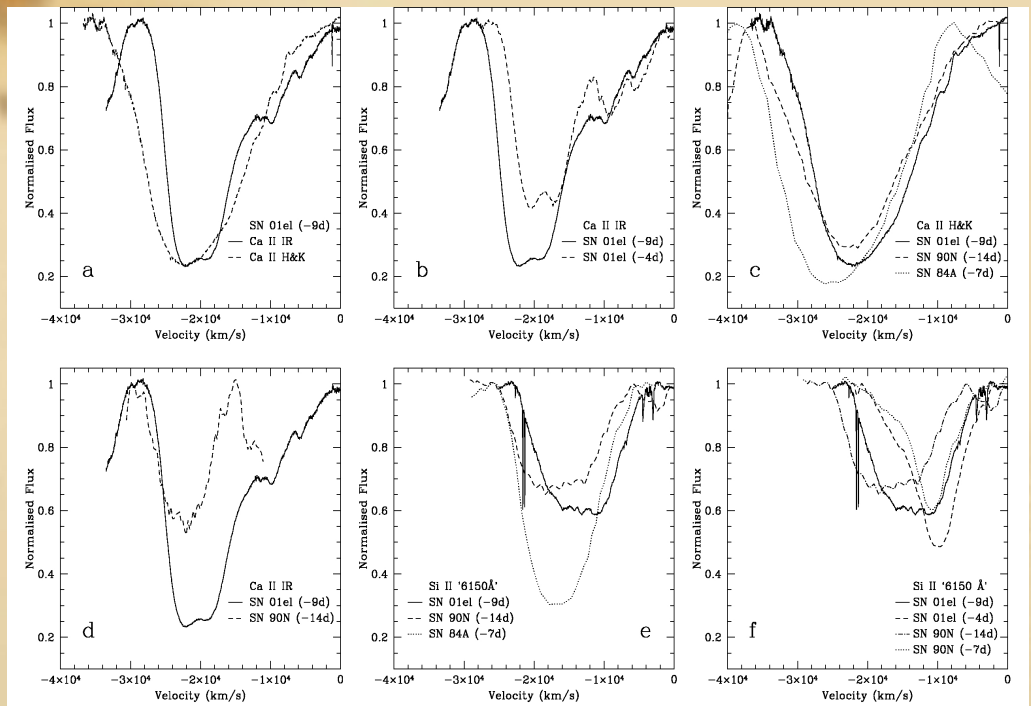

Fig. 8. a) Comparison between the Ca II IR triplet (solid line) and the Ca II H&K velocity profiles (dashed line) at −9 days. **b)** Spectral evolution of the Ca II IR triplet from −9 days (solid line) to −4 days (dashed line). **c)** The Ca II H&K profiles in SNe 2001el at −9 days (solid line), 1984A at −7 days (dotted line), and SN 1990N at −14 days (dashed line). **d)** Comparison between the Ca II IR triplet profiles of SNe 2001el (solid line) and 1990N (dashed line). Note that due to the limited wavelength coverage in SN 1990N spectrum the normalisation of its Ca II IR profile is unreliable in the red part. **e)** Comparisons between the Si II "6150 Å" profiles in SNe 2001el at −9 days (solid line), 1984A at −7 days (dotted line), and SN 1990N at −14 days (dashed line). **f)** Spectral evolution of the Si II "6150 Å" profile in SNe 2001el (solid and dashed lines) and 1990N (dotted and dotted-dashed lines). The flux calibrated (f_λ) spectral features have been normalised and converted to velocity space w.r.t. to the rest wavelengths assuming V_{rec} = 1180, 1010, and −261 km s^{-1} for SNe 2001el, 1990N, and 1984A, respectively. For this we used the rest wavelengths of the bluest components of the Ca II triplet/doublet lines viz. 8498 Å and 3934 Å, and the Si II "6150 Å" profile of 6347 Å.

Table 4. Maximum velocities for SNe 1984A, 1990N, and 2001el as indicated by the blue edges of the Ca II H&K and IR triplet and Si II "6150 Å" profiles (see Fig. 8).

SN	Epoch (days)	$V_{\text{Ca II,H\&K}}$ (km s^{-1})	$V_{\text{Ca II,IR}}$ (km s^{-1})	$V_{\text{Si II}}$ (km s^{-1})
1984A	−7[a]	38 000	–	26 000
1990N	−14[b]	36 000	~28 000	26 000
2001el	−9	34 000	28 000	23 000

[a] Date of observation 1984 Jan. 10 (Wegner & McMahan (1987). The epoch adopting Jan. 17 for the *B*-band maximum light (Barbon et al. 1989).
[b] Date of observation 1990 June 26.2 UT (Leibundgut et al. 1991).

We require: $V_{ej,max} \geq 4.5 \times 10^4$ km/s at 1 day (decays with time as $\propto t^{-0.2}$)

Early and late time VLT spectroscopy of SN 2001el – progenitor constraints for a type Ia supernova⋆

S. Mattila[1], P. Lundqvist[1], J. Sollerman[1], C. Kozma[1], E. Baron[2], C. Fransson[1], B. Leibundgut[3], and K. Nomoto[4]

[1] Stockholm Observatory, AlbaNova, Department of Astronomy, 106 91 Stockholm, Sweden
e-mail: seppo@astro.su.se
[2] Department of Physics and Astronomy, University of Oklahoma, 440 West Brooks Street, Norman, OK 73019, USA
[3] European Southern Observatory, Karl-Schwarzschild-Strasse 2, 85748 Garching bei München, Germany
[4] Department of Astronomy and Research Center for the Early Universe, University of Tokyo, Bunkyo-ku, Tokyo, Japan

Received 20 January 2005 / Accepted 26 September 2005

Modeling:

- Calculating the ionizing radiation from the reverse shock in detail, and in some models including the photospheric emission (from Blinnikov & Sorokina). Other contributions omitted. Models for $T_e = T_i$ and $T_e \neq T_i$ of the reverse shock have been made.
- Calculating the temperature and ionization structure of the unshocked circumstellar gas time dependently. (Elements included are H, He, C, N, O, Ne, Na, Mg, Al, Si, S, Ar, Ca and Fe. Most of the ions are treated as multilievel atoms.)
- Calculating the emission of the escaping line photons.

X-ray emission and absorption

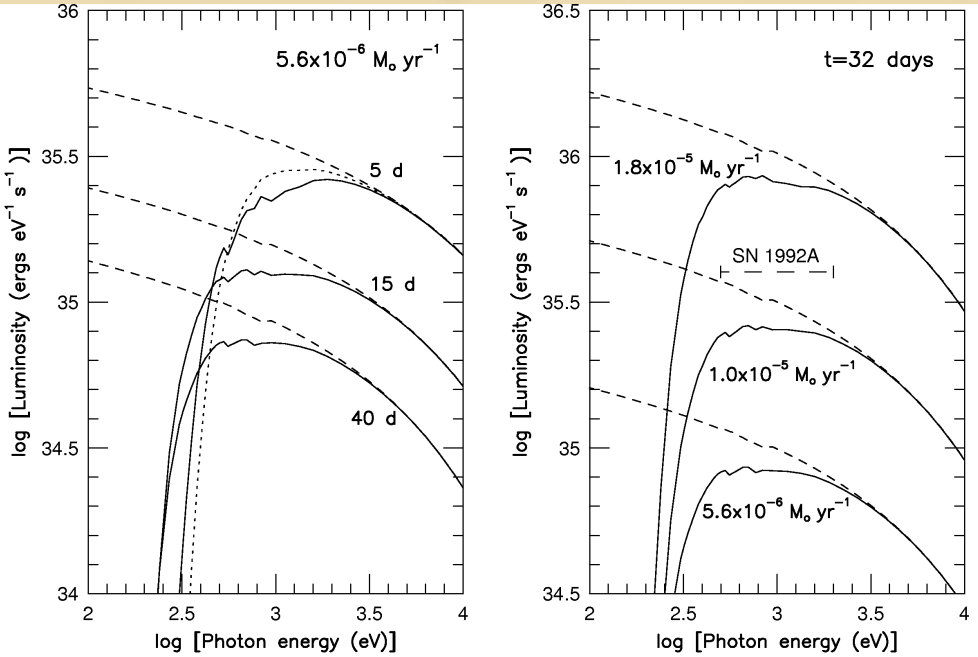

Fig. 9. Left: Ionizing spectrum at 5, 15 and 40 days for a model with a wind density described by the mass loss rate 5.6×10^{-6} $M_\odot$ yr^{-1} and wind speed 10 km s^{-1}. Ion and electrons in the shocked supernova ejecta are assumed to have the same temperature. Dashed lines show the unattenuated spectrum, while solid lines show the spectrum after absorption in the wind. (Dotted line shows a case for 5 days assuming He/H = 1.0. The other models have He/H = 0.085.) **Right:** Ionizing spectrum at 32 days for three mass loss rates (using the same representations as in the figure to the left). The vertical long-dashed bar shows the upper limit on the luminosity within 0.5 – 2.0 keV estimated by Schlegel & Petre (1993) for SN 1992A at $\sim$ 16 days after maximum. (For simplicity, we have assumed a constant flux within the passband used by Schlegel & Petre.)

Revised limit on mass loss rate for SN 1992A: <1.3x10^{-5} M$_o$/yr (for 10 km/s) (Lundqvist et al. 2008)

Chandra X-ray observations of SN 2002bo

(Hughes et al., 2007)

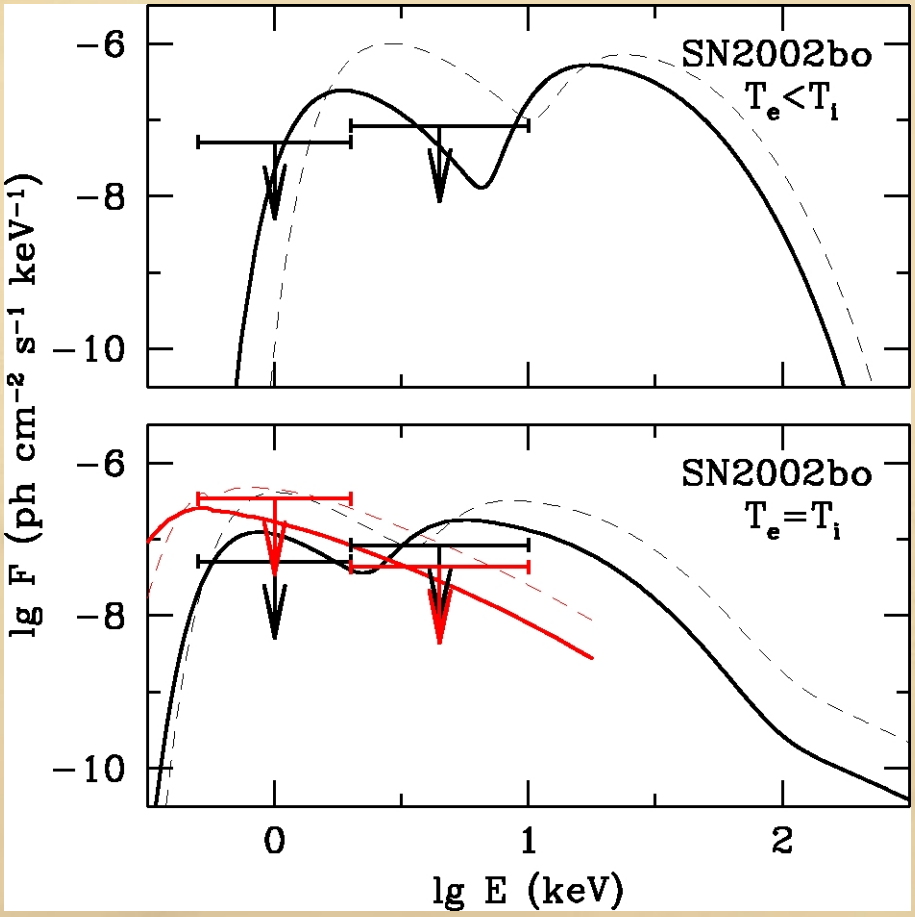

”Red” models are the same as in Lundqvist et al. (2008). Other models are described In Hughes et al. (2007). Mass loss rate limit is the same as the revised one for SN 1992A.

Optical campaigns were launched in 2000 using echelle spectrographs at VLT and Subaru.

Early Evolution of Nearby Type Ia Supernovae

(Probing the nature of the progenitors of thermonuclear supernovae)

ESO runs

(ESO Period 65 run: April 1, 2000 - September 30, 2000)
(ESO Period 66 run: October 1, 2000 - March 31, 2001)
(ESO Period 67 run: April 1, 2001 - September 30, 2001)
(ESO Period 68 run: October 1, 2001 - March 31, 2002)
(ESO Period 69 run: April 1, 2002 - September 30, 2002)
(ESO Period 70 run: October 1, 2002 - March 31, 2003)
(ESO Period 71 run: April 1, 2003 - September 30, 2003)
(ESO Period 72 run: October 1, 2003 - March 31, 2004)
(ESO Period 73 run: April 1, 2004 - September 30, 2004)
(ESO Period 75 run: April 1, 2005 - September 30, 2005)

Investigators: P. Lundqvist (PI), S. Mattila, J. Sollerman, E. Baron, P. Ehrenfreund, C. Fransson, B. Leibundgut, K. Nomoto & The SN Ia RTN team

Subaru runs

(Subaru Semester S04A run: April 1, 2004 - September 30, 2004)
(Subaru Semester S04B run: October 1, 2004 - March 31, 2005)
(Subaru Semester S05A run: April 1, 2004 - August 31, 2005)

Investigators: P. Lundqvist (PI), S. Mattila, K. Nomoto, J. Sollerman, H. Ando, J. Deng, P. Ehrenfreund, C. Fransson, R. Kotak, K. Maeda, A. Tajitsu, H. Terada

Last updated - June11, 2005
by Peter Lundqvist, peter@astro.su.se

For a smooth r^{-2} wind it is important to do very early observations. One could then reach down to a few x 10^{-6} M_o/yr for a supernova within 20 Mpc.

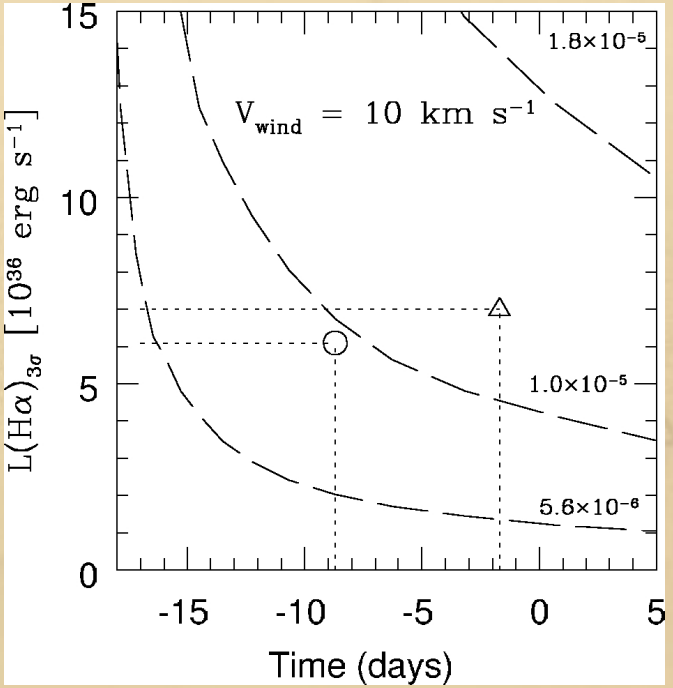

(Mattila et al. 2005)

Results from the optical observations (SN 2000cx)

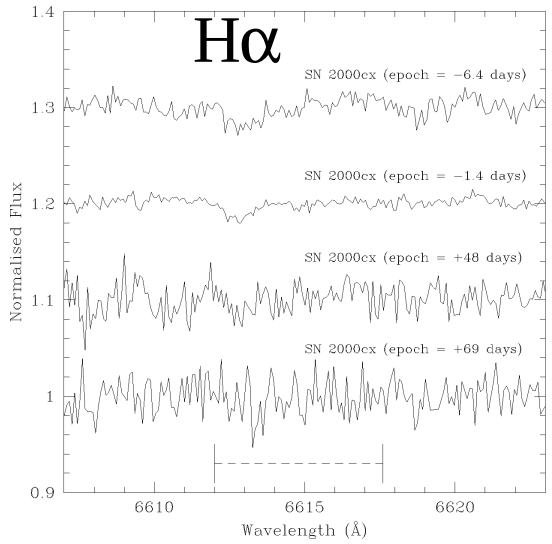

Fig. 1. Normalized UVES spectra in the expected spectral region around Hα for SN 2000cx on four epochs July 20.3, July 25.3, September 3.2, and October 12.3 (UT) 2000. The expected wavelength range of Hα is marked with a horizontal dashed line. No signs of CS Hα lines are visible either in emission or absorption (note that the feature at 6613 Å visible in the SN 2000cx spectra has been identified to be due to instrumental/atmospheric effects).

Table 2. 3σ upper limits on CS emission line fluxes of SN 2000cx. (Fluxes are not dereddened.)

Julian day (24500+)	epoch[a] (days)	line	FWHM (km s^{-1})	flux (ergs s^{-1} cm^{-2})
1745.8	−6.4	Hα	37[b]	8.4(−17)[c]
		Hα	62[d]	1.3(−16)
		Hα	106[e]	1.5(−16)
		Hα	203[f]	2.3(−16)
		He I[g]	21[b]	7.2(−17)
		He I[g]	53[d]	1.1(−16)
		He II[h]	21[b]	4.7(−17)
		He II[h]	53[d]	7.9(−17)
1750.8	−1.4	Hα	37[b]	8.7(−17)
		Hα	62[d]	1.4(−16)
		He I[g]	21[b]	7.2(−17)
		He I[g]	53[d]	1.3(−16)
		He II[h]	21[b]	4.0(−17)
		He II[h]	53[d]	7.7(−17)
1799.7	+47.5	Hα	37[b]	3.1(−17)
		Hα	62[d]	4.8(−17)
1820.7	+68.5	Hα	37[b]	1.3(−17)
		Hα	62[d]	1.7(−17)
		Hα	106[e]	2.0(−17)
		Hα	203[f]	3.0(−17)

[a] Relative to B-band maximum (JD2451752.2, Li et al. 2001). To obtain the time since explosion used in, e.g., Figs. 11 and 12, a rise time of 16 days was assumed (as found for SN 1994D in Riess et al. 1999).
[b] Assuming $T = 2.8 \times 10^4$ K and $v = 10$ km s^{-1} for the wind.
[c] 9.2(−17) stands for 9.2×10^{-17}.
[d] Assuming $T = 2.8 \times 10^4$ K and $v = 50$ km s^{-1} for the wind.
[e] Assuming $T = 2.8 \times 10^4$ K and $v = 100$ km s^{-1} for the wind.
[f] Assuming $T = 2.8 \times 10^4$ K and $v = 200$ km s^{-1} for the wind.
[g] He I λ5876
[h] He II λ4686

(Lundqvist et al. 2008)

SN 2000cx: helium lines

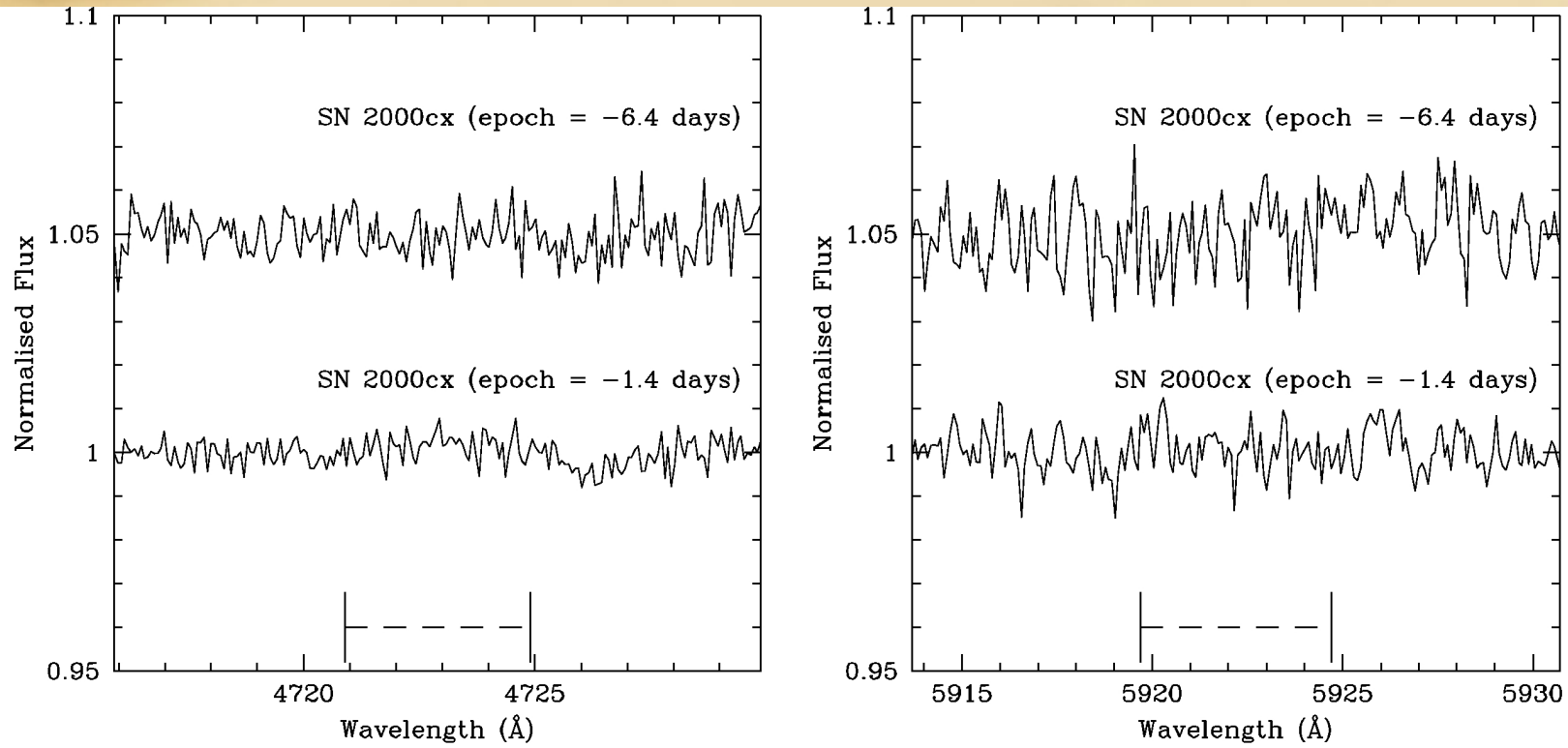

Fig. 2. Normalized UVES spectra in the expected spectral regions around He II λ4686 and He I λ5876) for SN 2000cx on two epochs July 20.3, July 25.3 (UT) 2000. The expected wavelength range of the CS line is marked with a horizontal dashed line. No signs of CS lines are visible either in emission or absorption.

(Lundqvist et al. 2008)

SN 2001el

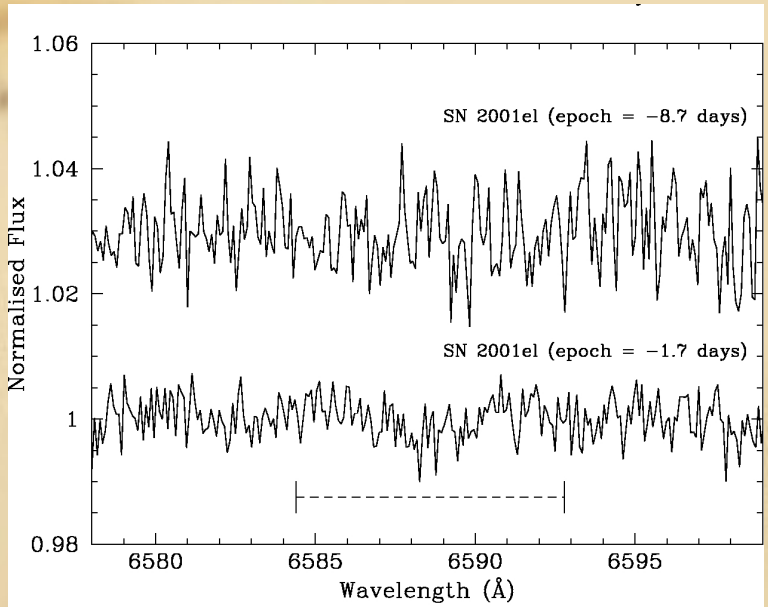

Fig. 3. Normalised and rebinned (~4 km s^{-1} $pixel^{-1}$) UVES spectra in the expected spectral region around Hα for SN 2001el on two epochs, September 21.3 and 28.3 (UT) 2001, i.e., 8.7 and 1.7 days before the SN maximum light, respectively. The expected wavelength range of Hα is marked with a horizontal dashed line, and the upper spectrum has been shifted vertically for clarity. No significant emission or absorption lines are visible.

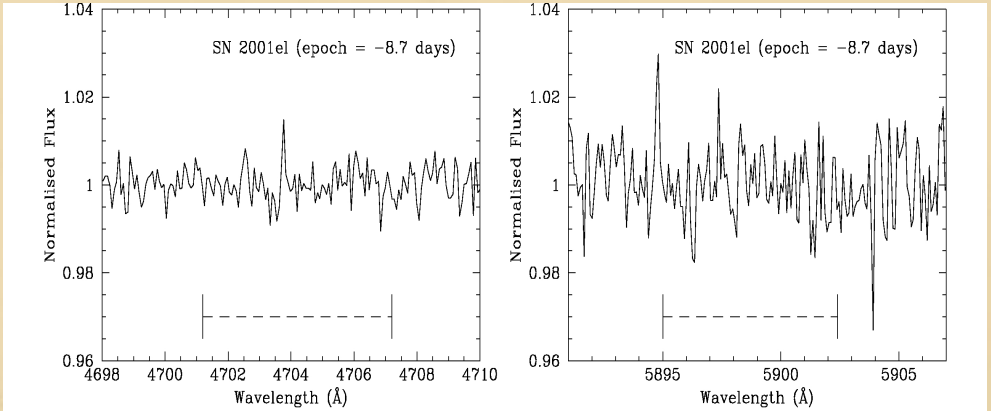

Fig. 4. Normalised and rebinned (~4 km s^{-1} $pixel^{-1}$) UVES spectra in the expected spectral regions around He II (4686 Å) and He I (5876 Å) for SN 2001el on September 21.3 (UT) 2001, i.e., 8.7 days before the maximum light. The expected wavelength range of the CSM lines is marked with a horizontal dashed line. No significant emission or absorption lines are visible.

Limit on mass loss rate: 9×10^{-6} M_o/yr (for a 10 km/s wind)

(Mattila et al. 2005)

Radio observations of SNe Ia

The Astrophysical Journal, 646:369–377, 2006 July 20

A SEARCH FOR RADIO EMISSION FROM TYPE Ia SUPERNOVAE

Nino Panagia,[1,2] Schuyler D. Van Dyk,[3] Kurt W. Weiler,[4] Richard A. Sramek,[5] Christopher J. Stockdale,[6] and Kimberly P. Murata[7]

Received 2006 February 21; accepted 2006 March 29

Using Chevalier's model From 1983 and adopting scaling of emission from SNe Ib and Ic, **Panagia et al. (2006)** obtain very low upper limits on the wind density.

TABLE 3

Lowest Upper Limits to SN Ia Progenitor Mass-Loss Rates

SN (1)	Distance (Mpc) (2)	Epoch (days) (3)	Wavelength (cm) (4)	Radio Luminosity[a] ($ergs^{-1}$ Hz^{-1}) (5)	$\dot{M}$[b] ($M_\odot$ yr^{-1}) (6)
1980N	23.3	71	6	2.5×10^{26}	1.1×10^{-6}
1981B	16.6	17	6	6.5×10^{25}	1.3×10^{-7}
1982E	23.1	1416	20	2.3×10^{26}	7.3×10^{-6}
1983G	17.8	71	6	5.0×10^{25}	4.1×10^{-7}
1984A	17.4	74	6	7.1×10^{25}	5.3×10^{-7}
1985A	26.8	55	20	1.2×10^{26}	2.5×10^{-7}
1985B	28.0	69	20	3.1×10^{26}	6.1×10^{-7}
1986A	46.1	57	6	2.6×10^{26}	9.2×10^{-7}
1986G	5.5	28	6	5.0×10^{25}	1.7×10^{-7}
1986O	28	71	6	1.3×10^{26}	7.4×10^{-7}
1987D	30	83	6	1.3×10^{26}	8.4×10^{-7}
1987N	37.0	67	20	4.2×10^{26}	7.4×10^{-7}
1989B	11.1	15	3.6	8.1×10^{24}	3.3×10^{-8}
1989M	17.4	50	6	9.2×10^{25}	4.4×10^{-7}
1990M	39.4	32	3.6	1.5×10^{26}	5.4×10^{-7}
1991T	14.1	28	3.6	2.3×10^{25}	1.5×10^{-7}
1991bg	17.4	29	3.6	1.1×10^{26}	2.0×10^{-7}
1992A	24.0	29	6	4.1×10^{25}	1.6×10^{-7}
1994D	14	61	6	2.8×10^{25}	2.5×10^{-7}
1995al	30	17	20	1.7×10^{26}	1.2×10^{-7}
1996X	30	66	3.6	1.9×10^{26}	1.2×10^{-6}
1998bu	11.8	28	3.6	1.3×10^{25}	1.1×10^{-7}
1999by	11.3	15	3.6	2.1×10^{25}	8.0×10^{-8}
2002bo	22	95	20	6.8×10^{25}	3.0×10^{-7}
2002cv	22	41	20	6.8×10^{25}	3.0×10^{-7}
2003hv	23	61	3.6	6.2×10^{25}	5.8×10^{-7}
2003if	26.4	68	3.6	8.1×10^{25}	7.6×10^{-7}

[a] The spectral luminosity upper limit (2 σ), as estimated at the wavelength given in col. (4), which, when combined with the age of the SN at the time of observation, yielded the lowest mass-loss rate limit.

[b] The upper limit (2 σ) to the mass-loss rate, $\dot{M}$, is calculated from the spectral luminosity lowest upper limit given in col. (5), as measured at the wavelength given in col. (4) at an epoch after explosion given in col. (3). The mass-loss limits are calculated with the assumption that the SN Ia progenitor systems can be modeled by the known properties of SN Ib/c progenitor systems, and that the pre-SN wind velocity establishing the CSM is $w_{\rm wind} = 10\ {\rm km\ s^{-1}}$.

Radio program at ATCA

Australia Telescope Compact Array **2006OCTS / C1303**

Probing the radio emission from a young Type Ia supernova

Name	Email	Affiliation	Country	Student	At site?
Principal investigator					
Peter Lundqvist	peter@astro.su.se	Stockholm Observatory	Sweden	No	No
Co-Investigators					
Claes-Ingvar Bjornsson	bjornsso@astro.su.se	Stockholm Observatory	Sweden	No	No
Claes Fransson	claes@astro.su.se	Stockholm Observatory	Sweden	No	No
Brian Schmidt	brian@mso.anu.edu.au	Australia National University	Australia	No	No
Miguel Angel Perez-Torres	torres@iaa.es	IAA - C SIC / Instituto de Astrofisica de Andalucia	Spain	No	No
Stuart Ryder	sdr@aao.gov.au	Anglo-Australian Observatory	Australia	No	No

As radio observations do appear to be the most sensitive to detect smooth mass loss, we have since 2004 been using ATCA.

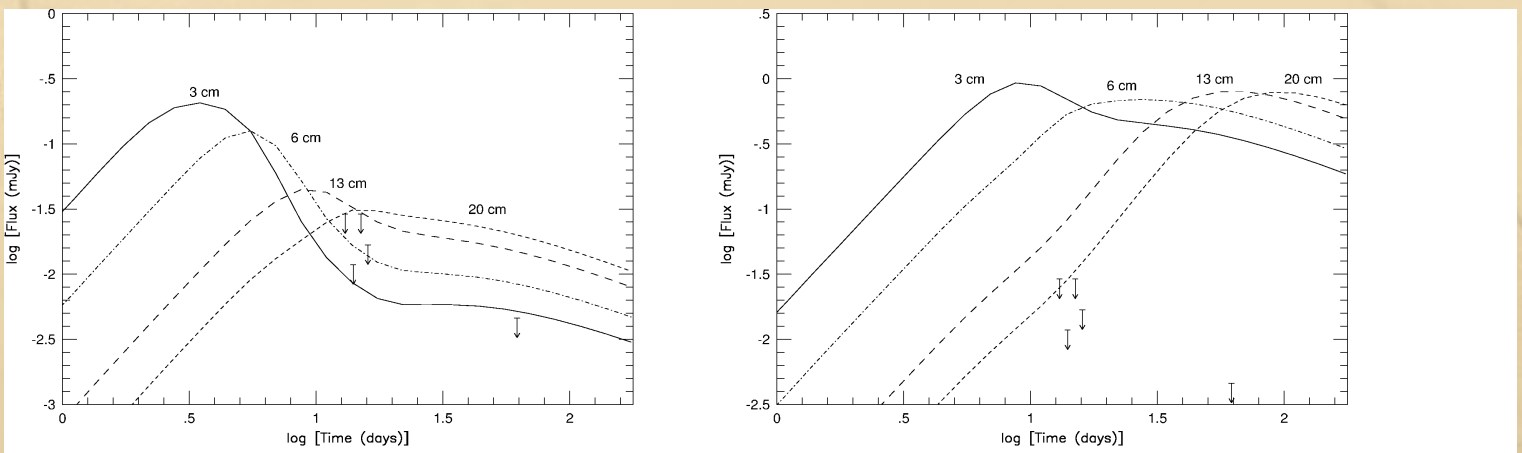

Figure 1: Radio light curves for a mass loss rate of 10^{-7} $M_\odot$ yr^{-1} (for $V_{\rm wind} = 10$ km s^{-1}) and two assumptions about the ratio of the energy densities of the magnetic field and relativistic electron density: 1% (left) and 10% (right). The expansion velocity on day 1 after explosion is $50,000$ km s^{-1}, and the ejecta density decreases as r^{-7} (e.g., Chevalier 1982). All cooling processes, like synchrotron and Compton cooling, are included. Note the earlier turn on of the flux for the lower efficiency case. The depression of the emission around 20 days at mainly high frequencies is due to Compton cooling. The distance to the modeled event is 20 Mpc. 3σ upper limits of observed events have also been included, after scaling for their actual distances: 1986G ($t = 13$ days, $\lambda = 2$ cm), 1998bu ($t = 14$ days, $\lambda = 3.6$ cm), 1989B ($t = 15$ days, $\lambda = 3.6$ cm), 1999by ($t = 16$ days, $\lambda = 3.6$ cm), and 1994D ($t = 62$ days, $\lambda = 6$ cm).

For the only SNe Ia displaying circumstellar *emission*, radio and X-rays have, however, failed to detect the SNe.

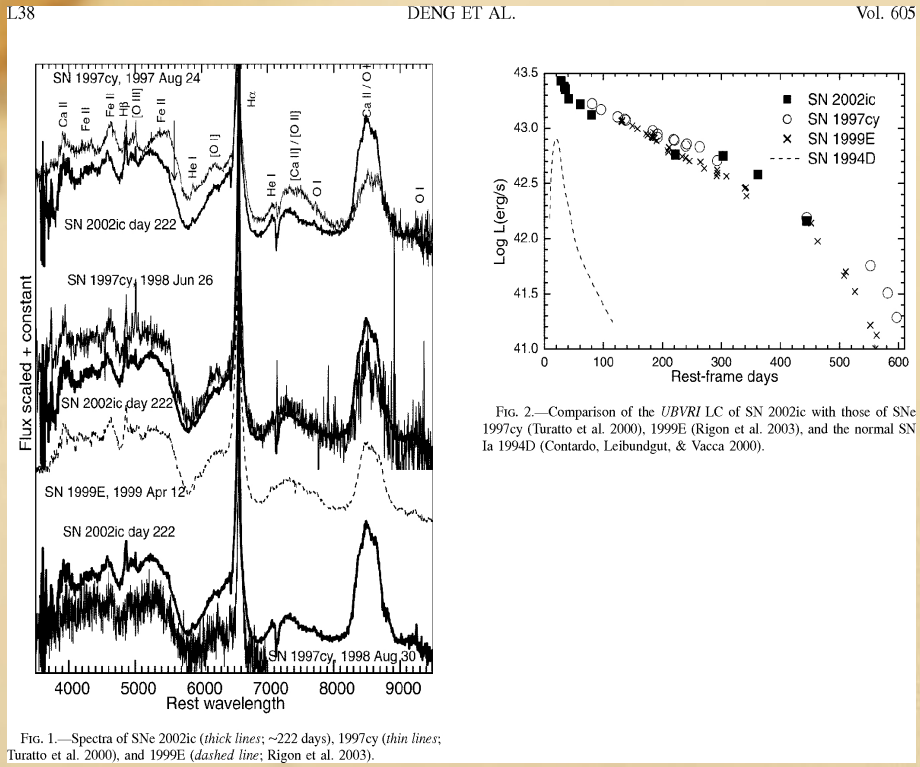

FIG. 1.—Spectra of SNe 2002ic (*thick lines*; ~222 days), 1997cy (*thin lines*; Turatto et al. 2000), and 1999E (*dashed line*; Rigon et al. 2003).

FIG. 2.—Comparison of the *UBVRI* LC of SN 2002ic with those of SNe 1997cy (Turatto et al. 2000), 1999E (Rigon et al. 2003), and the normal SN Ia 1994D (Contardo, Leibundgut, & Vacca 2000).

SN 2002ic (Deng et al. 2004)

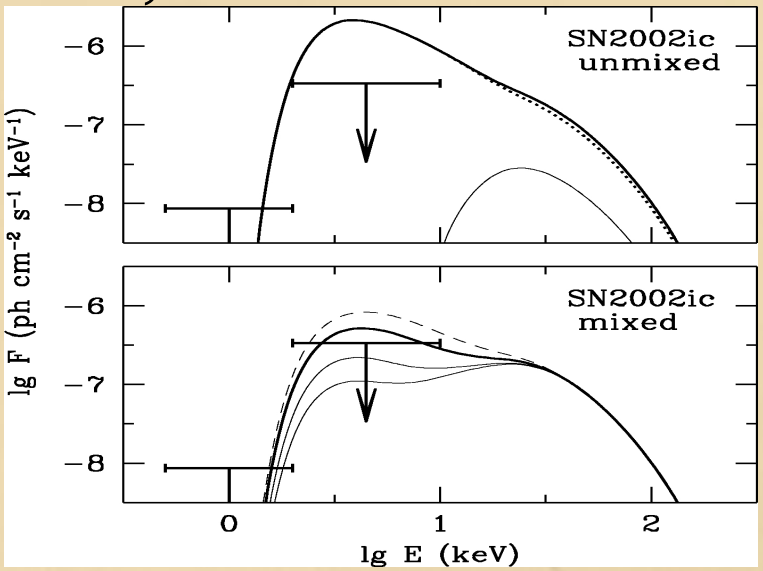

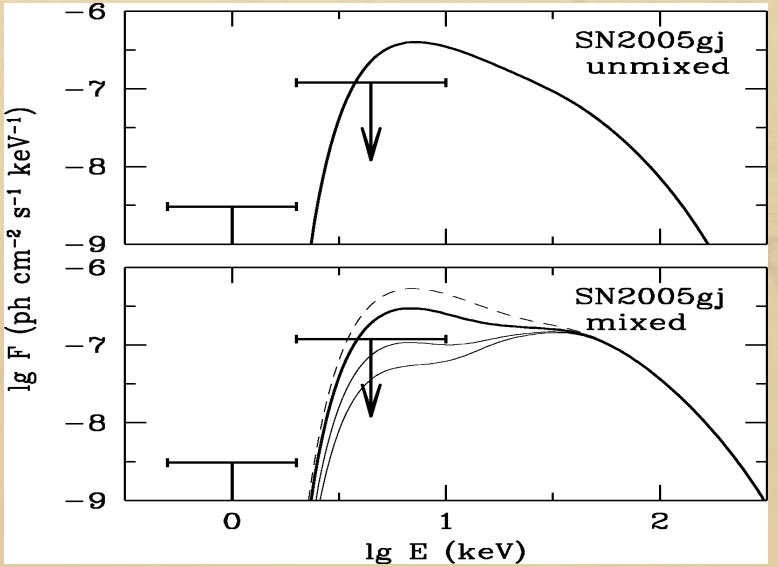

Chandra X-ray observations (Hughes et al. 2007)

Absorption features in SN 2006X.

(Patat et al., 2007)

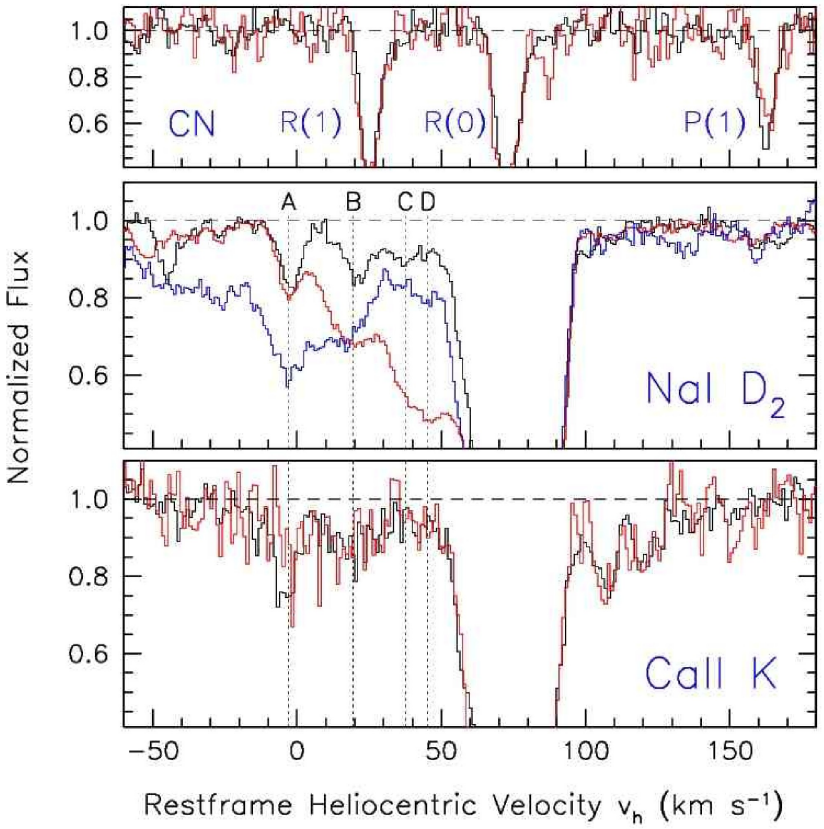

Figure 2: Evolution of the Na I D_2 and Ca II K line profiles between day -2 (black), day +14 (red) and day +61 (blue, Na I D_2 only). The vertical dotted lines mark the four main variable components at -3 (A), +20 (B), +38 (C) and +45 (D) km s^{-1}. For comparison, the upper panel shows the $R(0)$, $R(1)$ and $P(1)$ line profiles of the (0-0) vibrational band of the CN $B^2\Sigma - X^2\Sigma$. The velocity scale refers to the $R(0)$ transition (3874.608 Å). Color coding is as for the other two panels.

Absorption features in SN 2006X

- Patat et al.(2007) claim that the Na I variability is due to recombination in a shell at radius of about 10^{16} cm. The shell is then most likely circumstellar, and the mass loss rate is of order a few x 10^{-8} M_o/yr.
- Chugai (2008) has disputed this, and claims that the absence of Ca II 3934 Å gives an upper limit to the mass loss rate of 10^{-8} M_o/yr as (for v_{wind} = 30 km/s). The variable Na I lines do not come from gas closer to the star than 10^{17} cm. This gas does not have to be circumstellar.
- **Note:** Absence of Ca II (and Na I) lines could also be possible for relatively dense winds if the wind is kept ionized at Ca III (or higher), e.g., due to inverse Compton scattering. The absence of early radio emission, however, puts a limit on wind density which may argue against that. (Needs to be explored.)
- **Note also:** A shell around SN 2006X as discussed by Patat et al. should give rise to an X-ray/radio flash within a few months after the explosion.

Looking for hydrogen at late stages
Any signs of a non-degenerate companion?

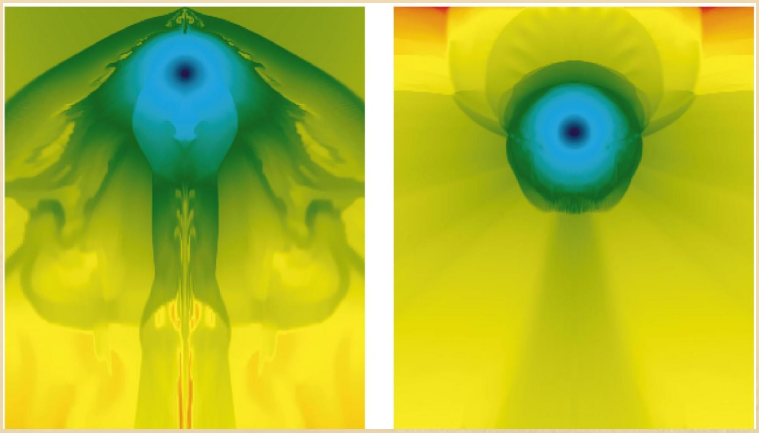

Simulations of a main sequence star being overtaken by the supernova ejecta **(Marietta et al. 2000)**

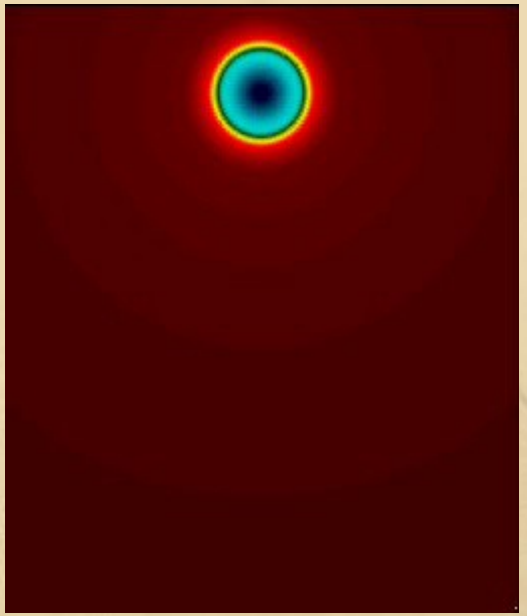

In no case, a faster than 10^3 km/s evaporation occurs. The material is deeply embedded in the SN ejecta and will not be seen until in the nebular phase.

Late emission modeling

We have used the same code as in Kozma et al. (2005)....

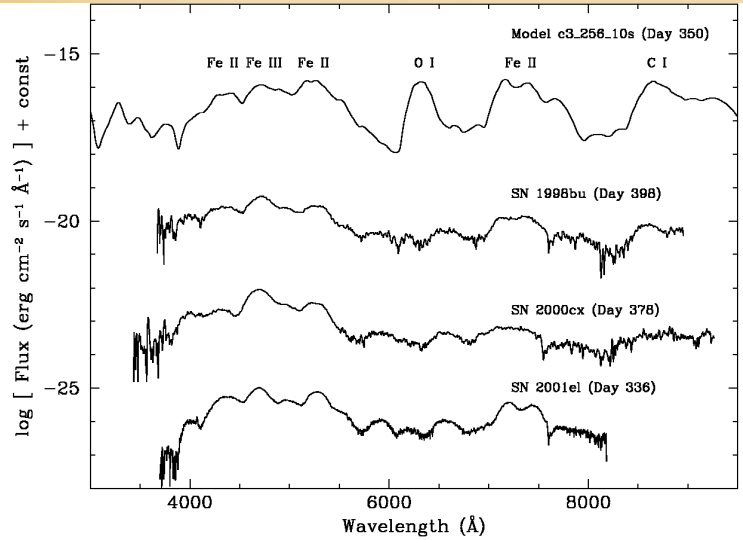

Fig. 5. Model spectrum at 350 days, for the c3_3d_256_10s model compared to observations of SN 1998bu from day 398, SN 2000cx from day 378, and of SN 2001el from 336 days after explosion. For clarity the observed spectra have been shifted relative to each other, the SN 1998bu spectrum by −4 dex, the SN 2000cx spectrum by −7 dex, and the SN 2001el spectrum by −10 dex. The observed spectra have been smoothed, dereddened, normalized to 350 days, and rescaled to a common distance of 10 Mpc as discussed in Sect. 3.1.

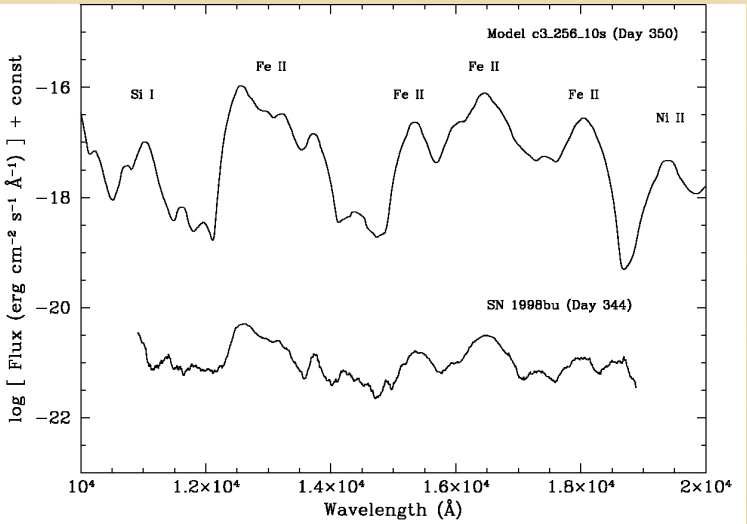

Fig. 6. Model IR spectrum at 350 days, for the c3_3d_256_10s model compared to observations of SN 1998bu from day 344 (Spyromilio et al. 2004). For clarity the observed spectrum has been shifted by −4 dex. The observations have been cleaned and heavily smoothed, using a Savitzky-Golay polynomial smoothing filter with a width of 50 wavelengthbins, corresponding to ~4500 km s^{-1}.

...although in our modeling we have used W7.
We have inserted solar abundance material within the innermost 10^3 km/s ejecta and compared with data.

SN 2000cx

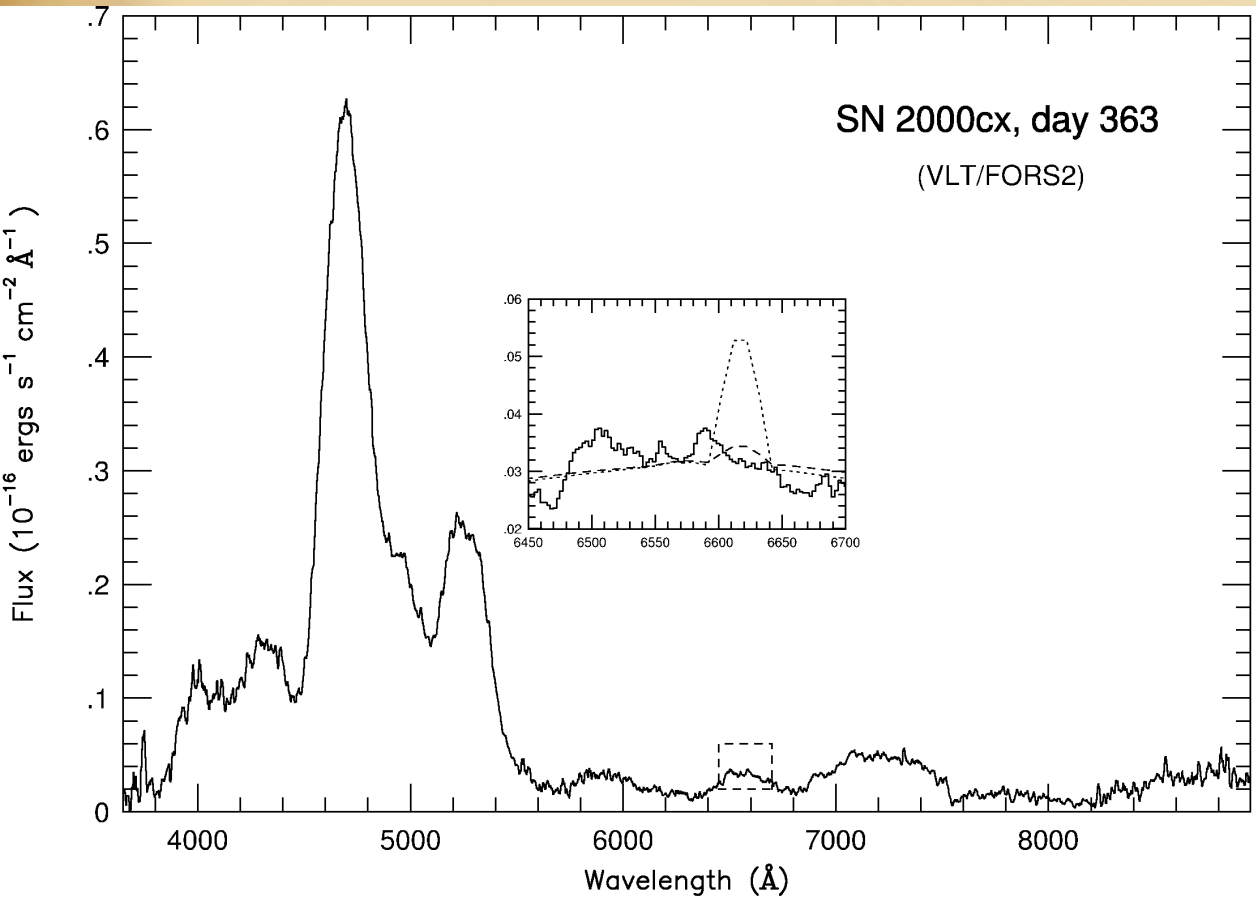

Fig. 6. VLT/FORS2 spectrum of SN 2000cx at 363 days after B maximum. The overall spectrum is described in Sollerman et al. (2004). The inset is a blow-up of the region marked by dashed lines, concentrating on wavelengths around Hα, i.e., ~ 6615 Å for the redshift of the supernova. The dashed and dotted spectra in the inset are models for the supernova, assuming 0.01 and 0.05 $M_\odot$ of solar abundance material, respectively, concentrated to $\pm 10^3$ km s^{-1} around the rest velocity of the supernova. This is to simulate Hα emission from gas removed from a possible companion star according to the models of Marietta et al. (2000). Our models for the Hα emission are described in the text. There is no sign of Hα emission in SN 2000cx at these wavelengths, which places a limit on low-velocity ($< 10^3$ km s^{-1}) hydrogen-rich material of ~ 0.03 $M_\odot$.

(Lundqvist et al. 2008)

SN 1998bu

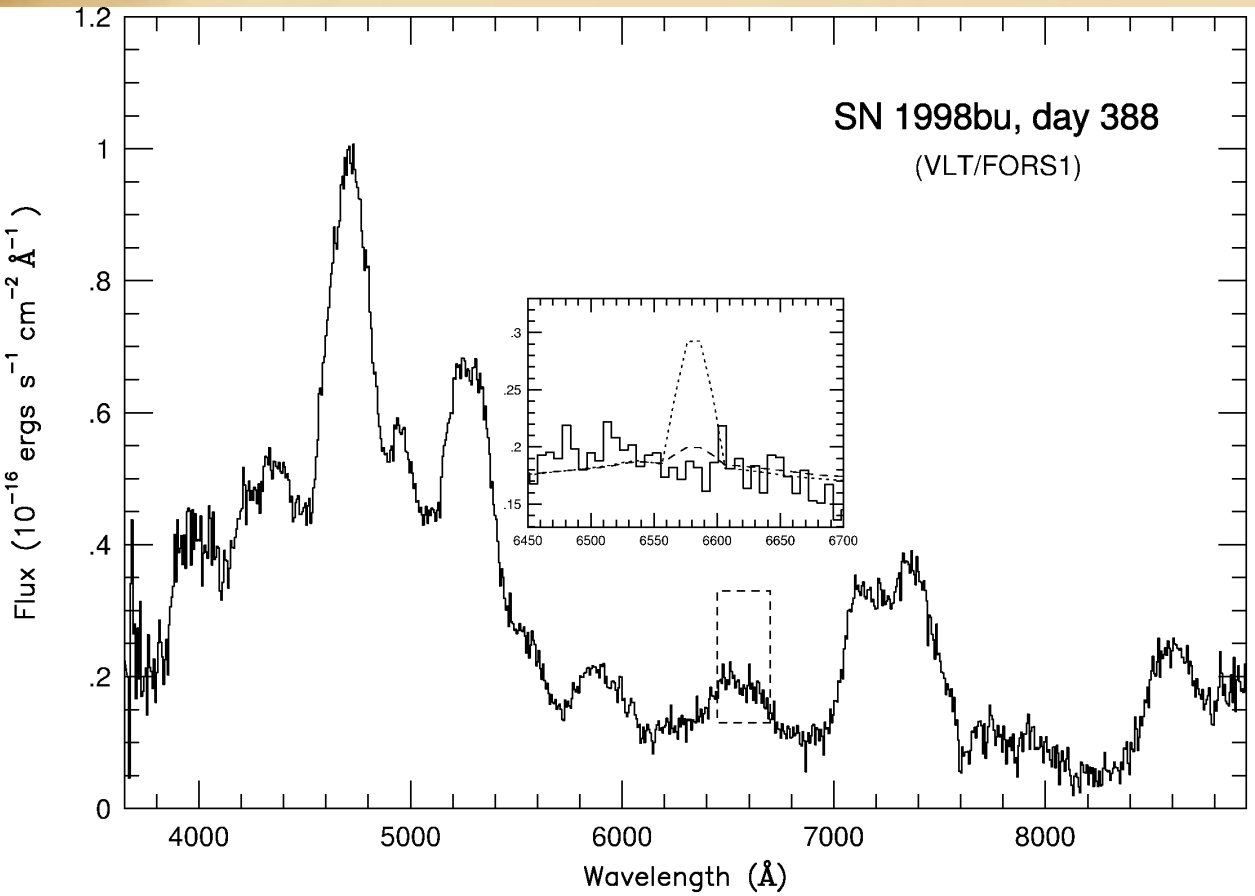

Fig. 7. VLT/FORS1 spectrum of SN 1998bu at 388 days after B maximum. The overall spectrum is very similar to the day 330 spectrum shown in Fig. 2 of Cappellaro et al. (2001), except for the stronger emission around 4000 Å, which is a result of a light echo from early emission. The inset is a blow-up of the region marked by dashed lines, concentrating on wavelengths around Hα. As in Fig. 6 we have plotted our model for Hα emission from a possible ablated companion star, and the mass within the core (i.e., $\pm 10^3$ km s^{-1}) is the same as in Fig. 6. We have assumed a distance to SN 1998bu of 11.2 Mpc, an extinction of $A_V = 1.0$ and a redshift of 750 km s^{-1} (Munari et al. 1998; Centurion et al. 1998). There is no sign of Hα emission in SN 1998bu at the expected wavelength. The day 388 VLT/FORS1 spectrum, and its implications for the light echo, is further discussed in Patat et al. (in preparation).

(Lundqvist et al. 2008)

SN 2001el

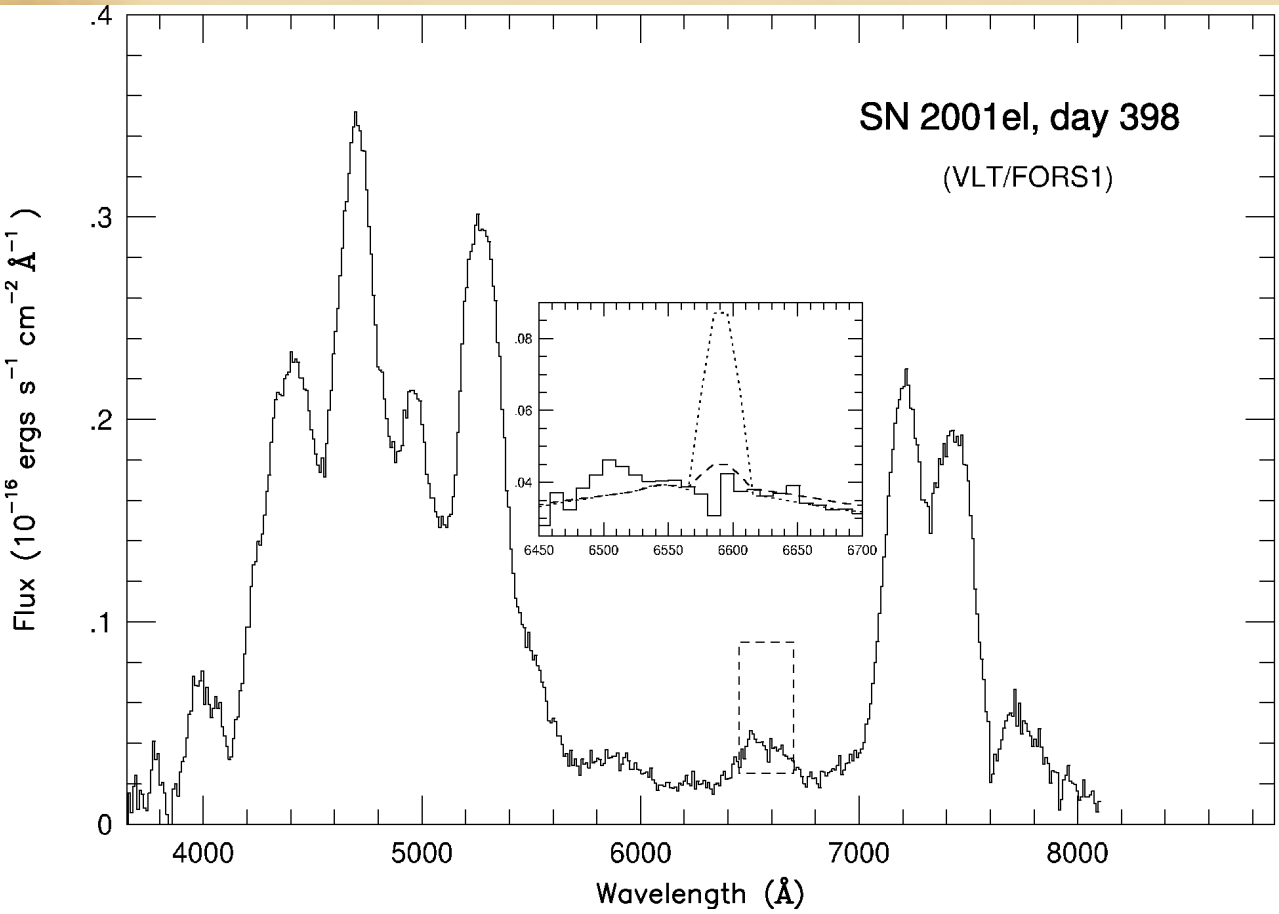

Fig. 6. FORS1 spectrum of SN 2001el obtained on November 2.2 (UT) 2002, i.e., 398 days past the *B*-band maximum light. The inset shows an enlargement of the region marked by dashed lines, focusing on wavelengths around Hα for the redshift of the SN. The SN emission at these wavelengths is dominated by a blend of Fe II emission lines (e.g., 6561 Å). The dashed and dotted spectra in the inset are models calculated at 380 days for the SN, assuming 0.01 $M_\odot$ and 0.05 $M_\odot$ of solar abundance material, respectively, concentrated to $\pm$1000 km s^{-1} from the rest velocity of the supernova. This is to simulate Hα emission from gas removed from a possible companion star according to the models of Marietta et al. (2000). There is no sign of such Hα emission in SN 2001el at these wavelengths, which places a limit on hydrogen rich material of ~0.03 $M_\odot$. The model used to calculate the late emission is described in Sect. 4.3.

(Mattila et al. 2008)

SN 1998bu in the near-IR

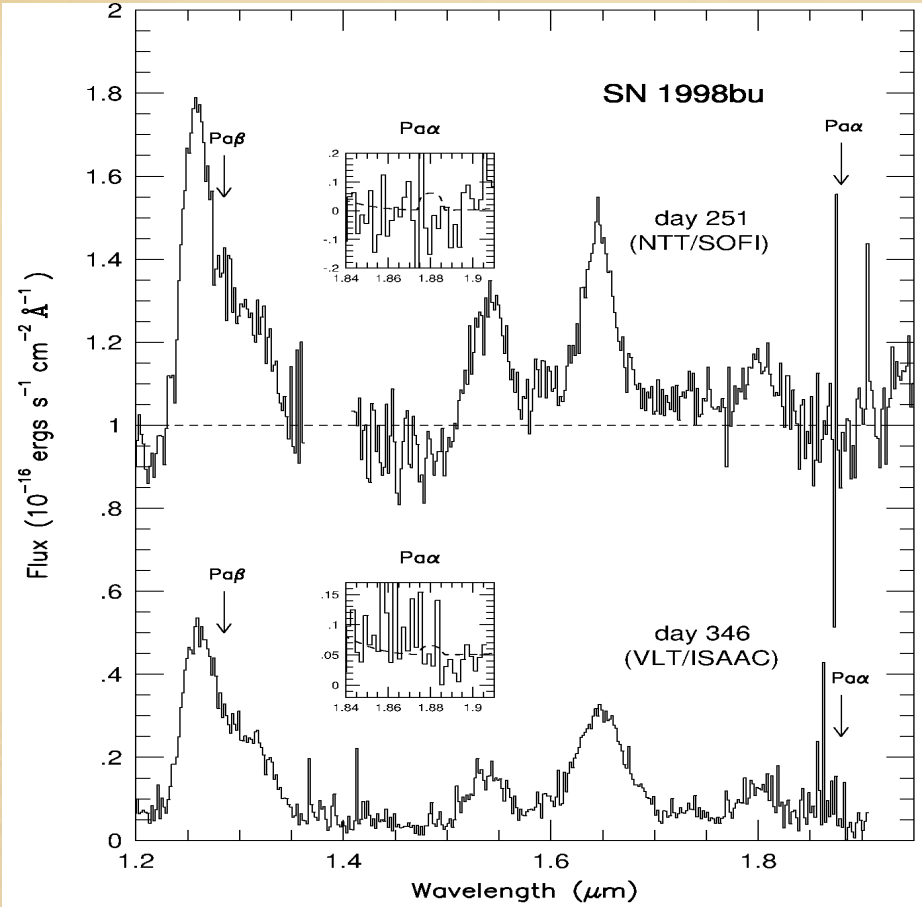

Fig. 8. Infrared spectra of SN 1998bu in the nebular phase taken at 251 days (ESO/NTT/SOFI) and 346 days (ESO/VLT/ISAAC) after B maximum. The arrows mark the rest wavelenghts of Paα and Paβ for SN 1998bu. The insets show blow-ups of the spectral region around Paα. The dashed spectrum is for a model discussed in Sect. 3.2 and displayed in Fig. 3 assuming 0.5 $M_\odot$ of hydrogen-rich material within the innermost $\pm 10^3$ km s^{-1} of the ejecta. This is to simulate the emission from the companion star in the models of Marietta et al. (2000). However, there is no sign of such Paα emission in SN 1998bu.

(Lundqvist et al. 2008)

SNe 2005am and 2005cf around Hα

(Leonard, 2007)

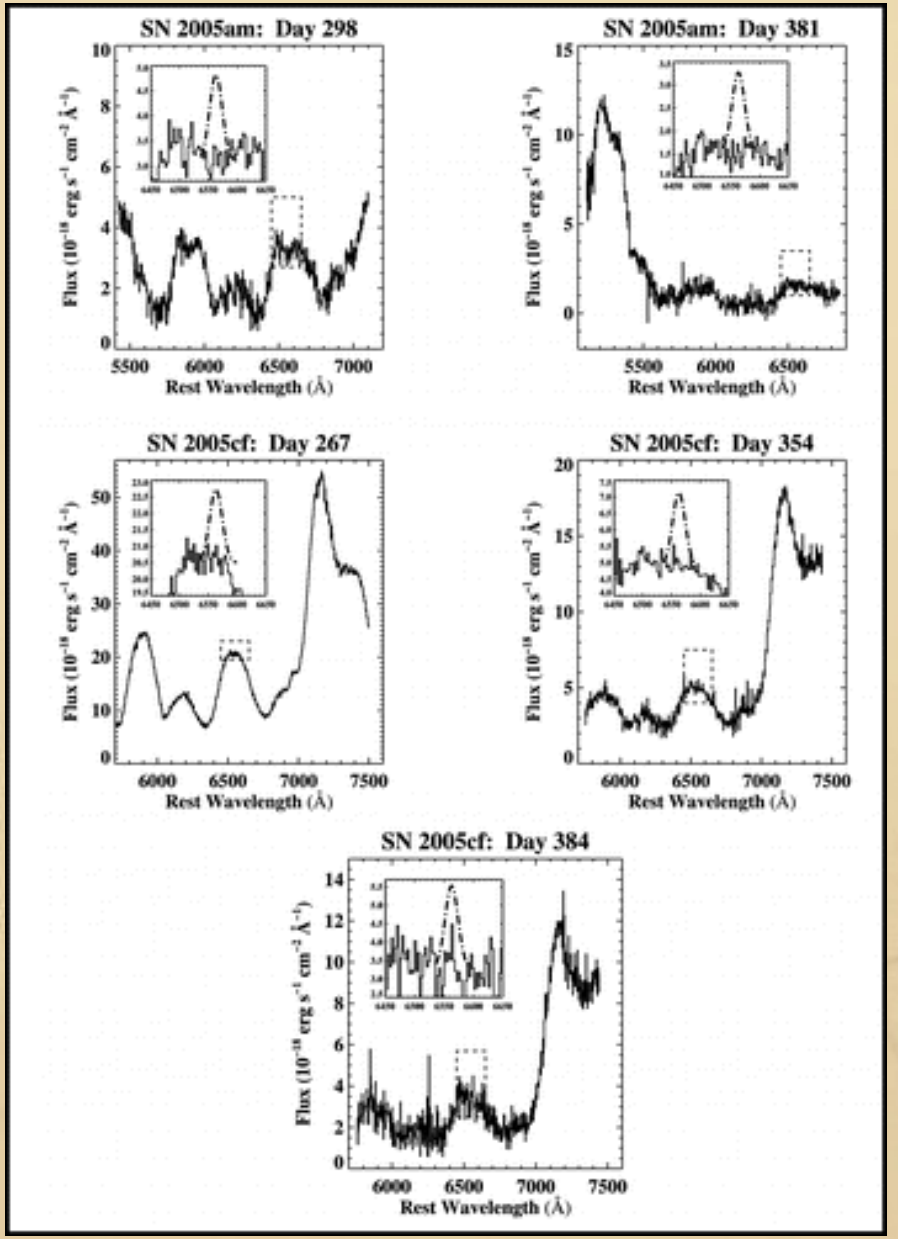

Late-time spectra of two SNe Ia, with day since B maximum indicated. The spectra are displayed at 3 Å bin^{+}, the approximate resolution at Hα. The expected strengths of the Hα line resulting from 0.05 $M_{\odot}$ of solar abundance material according to the day 380 models of Mattila et al.
(2005) are shown as dot-dashed lines in the insets; note that since the Hα emission is a time-dependent phenomenon, the estimated strength of these lines in the day 298 and day 267 spectra of SN 2005am and SN 2005cf, respectively, are only approximate.

An overview of which lines to expect

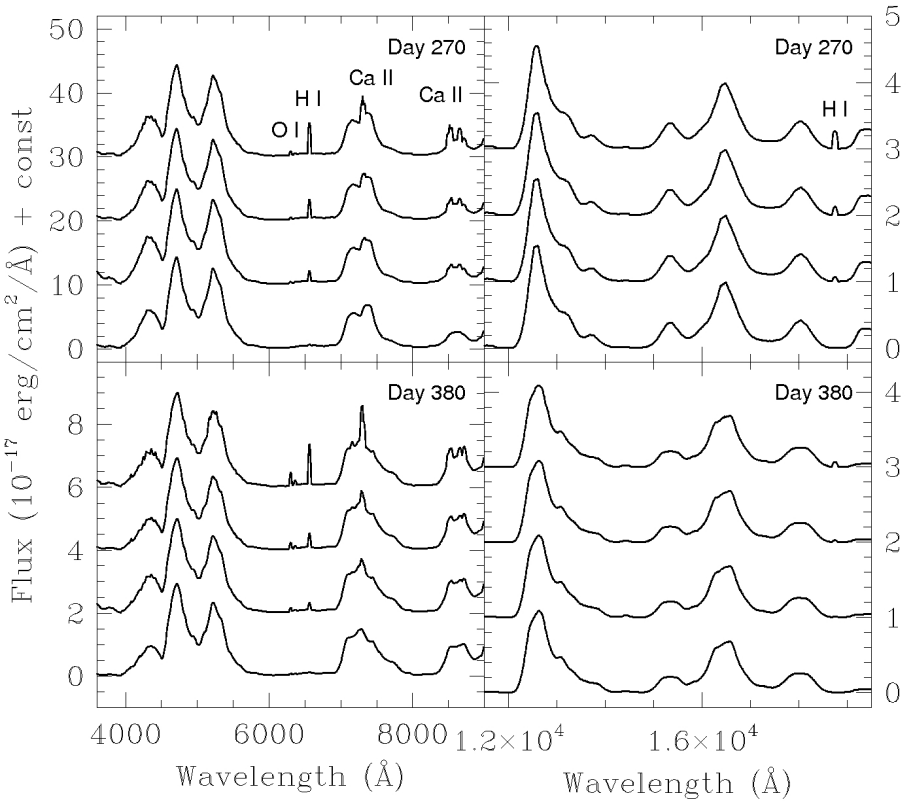

Fig. 13. Modeled spectra at two epochs, 270 and 380 days, for four models, with varying mass of the central, hydrogen rich region. The hydrogen mass increases from bottom to top in each frame, i.e., the lowest spectrum in each frame shows the model containg 0.01 $M_\odot$ of solar abundance matter, while the following spectra contain 0.05, 0.10, and 0.50 $M_\odot$, respectively. In these spectra we have also labeled the features originating in the hydrogen rich matter.

(Lundqvist et al. 2008)

Conclusions

- No detection of circumstellar *emission* from a ”normal” Type Ia SN has ever been seen in any wavelength region. Best limits are obtained in the radio and indicate $<10^{-7}$ M_o yr^{-1}. *Absorption* features in SN 2006X may not be due to circumstellar material. However, the absence of Ca II 3934Å absorption could indicate $<10^{-8}$ M_o yr^{-1}.

- Optical evidence for episodic mass loss exist for at least two suspected Type Ia SNe (SN 2002ic and SN 2005gj). Radio and X-ray emission was not detected (probably due to absorption by the circumstellar shell). The shells could be asymmetric.

- Late emission from five normal Type Ia SNe indicates that at most 0.03 M_o of solar abundance material exists in the center of any of these supernovae. This is much less than in any of the models calculated by Marietta et al. (2000) and puts constraints on single degenerate models. Have we included physics correctly? Helium-rich donor?

- Double degenerates pass all our tests for normal Type Ia SNe, and are also supported by the recent results by Totani et al. (2008).

Optical and near-IR lines (models compared to data.)

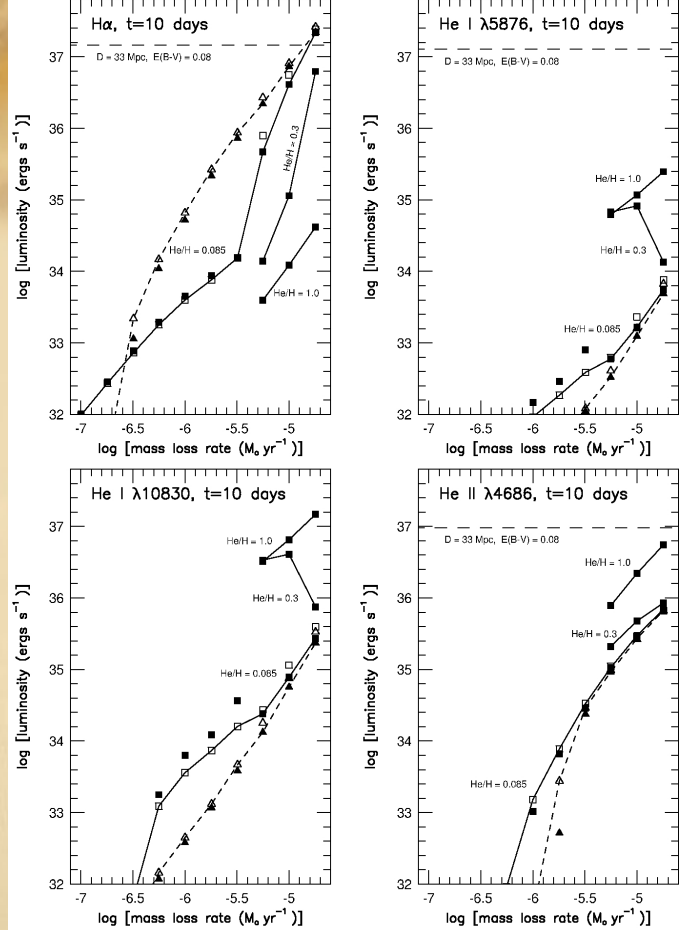

Fig. 11. Line luminosites at 10 days as a function of mass loss rate, assuming a wind speed of 10 km s^{-1}. Squares show models in which ionizing radiation is only produced by the reverse shock, while in models marked by triangles we have also included the photospheric emission from the model w7jzl155.ph of Blinnikov & Sorokina (2001). Filled symbols are for temperature equipartition between electrons and ions behind the reverse shock, whereas for open symbols $T_e = T_{rev}/2$. Models are shown for three values of the number density ratio He/H. The observed limit is for the first epoch in Table 2 for the case of a wind temperature of 2.8×10^4 K and a wind speed of 10 km s^{-1}. For SN 2000cx we have assumed a distance of 33 Mpc and an extinction of $E(B-V) = 0.08$. For further details, see text.

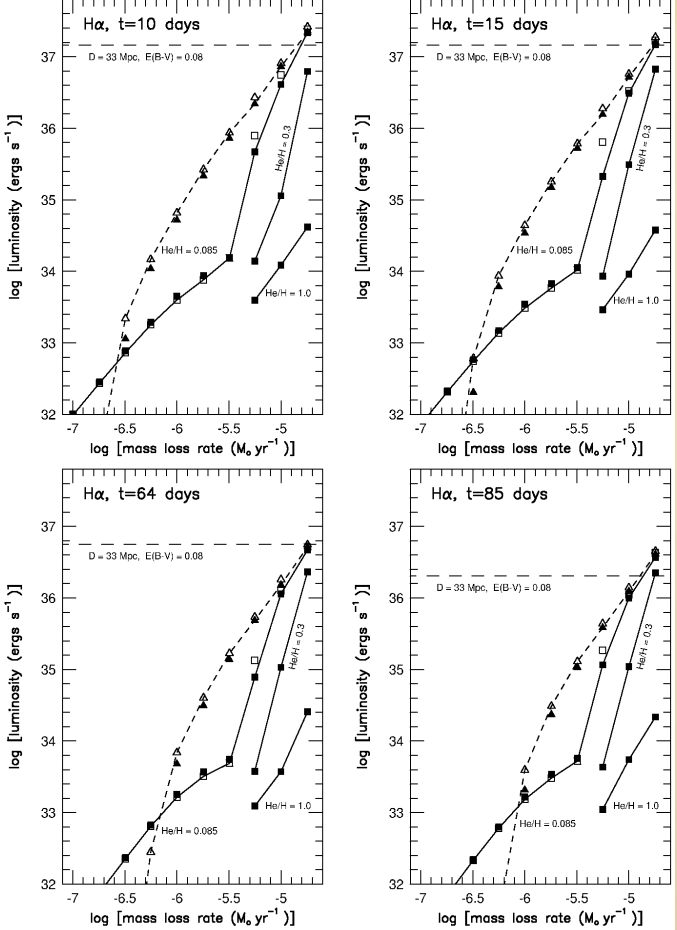

Fig. 12. Hα luminosity as a function of mass loss rate at four epochs corresponding to the epochs listed in Table 2 for SN 2000cx, assuming a wind speed of 10 km s^{-1}. The lines and symbols have the same meaning as in Fig. 11. The observed limits are for the four epochs in Table 2, assuming a wind temperature of 2.8×10^4 K and a wind speed of 10 km s^{-1}.

Data are for SN 2000cx (Lundqvist et al. 2008). Limit on mass loss rate is 1.2x10^{-5} M$_o$/yr for 10 km/s.